



Original Articles

A synergistic regulation works in matrix stiffness-driven invadopodia formation in HCC



Xi Zhang^{a,1}, Yingying Zhao^{a,1}, Miao Li^{a,1}, Mimi Wang^a, Jiali Qian^a, Zhiming Wang^b, Yaohui Wang^c, Fan Wang^d, Kun Guo^a, Dongmei Gao^a, Yan Zhao^a, Rongxin Chen^a, Zhenggang Ren^a, Haiyan Song^{e, **}, Jiefeng Cui^{a,*}

^a Liver Cancer Institute, Zhongshan Hospital, Fudan University & Key Laboratory of Carcinogenesis and Cancer Invasion of Ministry of Education, 180 Feng Lin Road, Shanghai, 200032, PR China

^b Department of Oncology, Zhongshan Hospital, Fudan University, Shanghai, 200032, PR China

^c Department of Radiology, Shanghai Cancer Center, Fudan University, Shanghai, 200032, PR China

^d Department of Oncology, Shanghai General Hospital, Shanghai Jiao Tong University School of Medicine, Shanghai, 200080, PR China

^e Institute of Digestive Diseases, Longhua Hospital, Shanghai University of Traditional Chinese Medicine, Shanghai, 200032, PR China

ARTICLE INFO

ABSTRACT

Keywords:

Matrix stiffness
Hepatocellular carcinoma (HCC)
Invadopodia
Integrin $\beta 1$
Piezo1

Growing evidence has suggested that increased matrix stiffness can significantly strengthen the malignant characteristics of hepatocellular carcinoma (HCC) cells. However, whether and how increased matrix stiffness regulates the formation of invadopodia in HCC cells remain largely unknown. In the study, we developed different experimental systems *in vitro* and *in vivo* to explore the effects of matrix stiffness on the formation of invadopodia and its relevant molecular mechanism. Our results demonstrated that increased matrix stiffness remarkably augmented the migration and invasion abilities of HCC cells, upregulated the expressions of invadopodia-associated genes and enhanced the number of invadopodia. Two regulatory pathways contribute to matrix stiffness-driven invadopodia formation together in HCC cells, including direct triggering invadopodia formation through activating integrin $\beta 1$ or Piezo1/FAK/Src/Arg/cortactin pathway, and indirect stimulating invadopodia formation through improving EGF production to activate EGFR/Src/Arg/cortactin pathway. Src was identified as the common hub molecule of two synergistic regulatory pathways. Simultaneously, activation of integrin $\beta 1$ /RhoA/ROCK1/MLC2 and Piezo1/ Ca^{2+} /MLCK/MLC2 pathways mediate matrix stiffness-reinforced cell migration. This study uncovers a new mechanism by which mechanosensory pathway and biochemical signal pathway synergistically regulate the formation of invadopodia in HCC cells.

1. Introduction

High migration and invasive ability are the remarkable characteristics of metastasizing cancer cells. The formation of invadopodia not only dominates the highly invasive biological behavior of cancer cells, but also acts as a critical molecular event to influence the process of invasion and metastasis [1,2]. Invadopodia appears as a F-actin-rich membrane protrusion structure [3,4]. Actin filament nucleators (F-actin core) and their surrounding regulatory proteins such as cortactin, the Arp2/3 complex, N-WASP and WASP-interacting protein are its basic components [5–7]. Traditional view holds that the formation of invadopodium

precursor is attributed to abnormal activation of driver genes Src and Ras [8,9], whereas recent evidence supports that driver mutations are not sufficient to alter the phenotype and biological behavior of cancer cells. Biochemical stimulation factors within tumor microenvironment, such as growth factors, ECM, intercellular contact, hypoxia, and exosomes, also play important roles in triggering phenotypic changes and invadopodia formation of cancer cells [10–13]. In addition to biochemical stimulation signals mentioned above, biomechanical stimulation signals within tumor microenvironment also seem to exert significant impacts on invadopodia formation [14]. Sporadic research reveals that high-stiffness stimulation obviously increases the number and activity of invadopodia in breast cancer cells through activating

* Corresponding author.

** Corresponding author.

E-mail addresses: songhaiyan@shutcm.edu.cn (H. Song), cui.jiefeng@zs-hospital.sh.cn (J. Cui).

¹ Xi Zhang, Yingying Zhao, Miao Li contributed to this study equally.

Abbreviations

AFP	Alpha Fetoprotein	IHC	Immunohistochemistry
ALB	Albumin	ITGB1	Integrin $\beta 1$
ALP	Alkaline Phosphatase	LOX	Lysyl Oxidase
ALT	Alanine Aminotransferase	MLC	Myosin Light Chain
APTT	Activated Partial Thromboplastin Time	MLCK	Myosin Light Chain Kinase
AST	Aspartate Aminotransferase	MMP14	Matrix Metalloprotein 14
CB	Conjugated Bilirubin	MVI	Microvascular Invasion
COL1A1	Collagen Type I Alpha 1 Chain	PBS	Phosphate Buffer Solution
Ctrl	Control	PCR	Polymerase Chain Reaction
DAB	Diaminobenzidine	PFS	Progression Free Survival
DMEM	Dulbecco Modified Eagle Medium	PI3K	Phosphoinositide-3-Kinase
ECM	Extracellular Matrix	PT	Prothrombin Time
EGF	Epidermal Growth Factor	PVDF	Polyvinylidene Fluoride
EGFR	Epidermal Growth Factor Receptor	qRT-PCR	Quantitative Real-time Polymerase Chain Reaction
EMT	Epithelial-Mesenchymal Transition	ROCK	Rho-associated Kinase
FAK	Focal Adhesion Kinase	SDS	Sodium Dodecyl Sulfate
FBS	Fetal Bovine Serum	TB	Total Bilirubin
FN	Fibronectin	TCGA	The Cancer Genome Atlas
GGT	γ -glutamyltransferase	TGF	Transforming Growth Factor
GLU	Glucose	Tyr	Tyrosine
HCC	Hepatocellular Carcinoma	WASP	Wiskott-Aldrich Syndrome Protein
HSC	Hepatic Stellate Cell	WT	Wild Type
		YAP	Yes-associated Protein

myosin II-FAK/Cas pathway [15], also intensifies invadopodia activity in head and neck squamous cell carcinoma and breast cancer via activating Rho/ROCK signaling pathway [16], indicating that there may be a close association between matrix stiffness and invasion ability of cancer cells. Stiffness of tumor tissue is usually higher than that of corresponding normal tissue [17]. Similar to other types of solid tumors, HCC also has a typical biomechanical feature of matrix stiffening. Clinically, increased matrix stiffness, which always occurs in the development and progression of HCC, is strongly associated with lower pathological grade and unfavorable prognosis [18,19]. Liver stiffness as a predictor has currently been used to assess HCC development and prognosis [20]. Despite the clinical significance of matrix stiffness in HCC progression has been well characterized, its regulatory mechanism still cannot be thoroughly understood due to the lack of ideal stiffness-related experimental systems. With construction and development of *in vivo* and *in vitro* stiffness-related experiment systems, a series of new findings about matrix stiffness-mediated effects on HCC have been gradually proposed from us and other research teams, including driving EMT occurrence independently [21,22], promoting angiogenesis [23–25] facilitating lung pre-metastatic niche formation [26–28], enhancing stemness characteristics [29], upregulating metastasis-associated gene expression [30], modulating vesicular trafficking and exosome secretion [31,32], impairing ferroptosis and anti-tumor immunity [33], affecting lipid metabolic reprogramming [34] and participating in chemotherapy resistance [18,35,36]. These findings sufficiently validate that increased matrix stiffness indeed strengthens malignant characteristics of HCC cells and promote their invasion and metastasis. However, little is known about whether and how increased matrix stiffness participates in or regulates the formation of invadopodia in HCC.

Chakraborty reports that the expression and secretion of Agrin promotes the formation of arp2/3 complex -dependent invadopodia [37], and Agrin-caused ECM/tissue stiffness effectively contribute to HCC progression [38], indicating a potential linkage between matrix stiffness and invadopodia formation in HCC. Besides, high-stiffness stimulation significantly alters the morphological phenotype of HCC cells, enhances their migration ability and F-actin polymerization, as well as metastasis-associated gene expression [21]. So increased matrix stiffness

is very likely to be an initial factor to trigger the formation of invadopodia in HCC cells. On the other hand, activated HSCs as a key driver contributes to ECM remodeling, matrix stiffening and HCC progression [39,40], and high-stiffness stimulation often result in the sustained activation of HSCs [40]. Accordingly, we speculate that biomechanical stimulation signals and paracrine-produced biochemical signals from HSCs may synergistically regulate the formation of invadopodia.

In this study, we developed different experimental systems *in vitro* and *in vivo* to explore the effects of matrix stiffness on the formation of invadopodia and its relevant molecular mechanism. Our results uncovered a new mechanism by which mechanosensory pathway and biochemical signal pathway synergistically regulated the formation of invadopodia in HCC. This discovery will be beneficial for updating and enriching the theory of matrix stiffness-regulated invadopodia, and giving new experiment evidence in HCC for establishing stiffness-targeted intervention strategy.

2. Materials and methods

2.1. Cells and cell culture

MHCC97H cells were obtained from the Liver Cancer Institute of Fudan University (Shanghai, China). Hep3B cells and hepatic stellate cells (LX-2) were purchased from the Cell Bank of Shanghai Institute of Biochemistry and Cell Biology (Shanghai, China). MHCC97H cells were cultured in Dulbecco's Modified Eagle's Medium (DMEM, Gibco, New York, NY, USA) supplemented with 10 % fetal bovine serum (FBS, Biowest, Riverside, MO, USA) and 1 % penicillin/streptomycin (Gibco), and Hep3B cells in Minimum Essential Medium (Gibco) with 12.5 % FBS and 1 % penicillin/streptomycin. LX-2 cells were grown in the same culture medium as MHCC97H cells.

2.2. *In vitro* system of FN-coated polyacrylamide gels with different stiffness

FN-coated polyacrylamide gels with stiffness of 6 kPa (low-stiffness), 10 kPa (medium-stiffness), and 16 kPa (high-stiffness) were established for cell culture as our previous study [28], and the culture and collection

of the cells on different stiffness substrates were performed as the procedure reported previously [23].

2.3. Lentivirus infection

The target fragments of human genes ITGB1 and PIEZO1 and packaging recombinant plasmid of lentivirus were designed and constructed in collaboration with GeneChem (Shanghai, China). In brief, shRNA for ITGB1 (ITGB1: 5'-CCTCCAGATGACATAGAAA-3'), PIEZO1 (81882: 5'-GCACCTCATTATGTTGAGGA-3'; 81883: 5'-GAAGACCA-CATTGAGGTGAA-3'; 81884: 5'-CCCTGTGCATTGATTATCCCT-3'), and scramble (5'-TTCTCCGAACGTGTCACT-3') were synthesized and cloned into the plasmid pGCSIL, respectively. When HCC cells grew and reached 40 % confluence, they were infected with lentivirus and selected by puromycin (2 µg/mL). The efficiency of inhibition was determined by qRT-PCR and Western blot.

2.4. Cell migration analysis of HCC cells grown on different stiffness substrates using a cell IQ cell workstation

Migration trajectories of HCC cells grown on different stiffness were recorded and analyzed in real time using a Cell IQ living cell workstation (Chip-Man Technologies, Tampere, Finland). Cells were continuously cultured in a living cell workstation for 48 h, and their migration trajectories were recorded through taking continuous photos every hour at the same location. A total of 40 cells were randomly selected in each group for statistical analysis. The Manual Tracking plug-in of ImageJ software and Chemotaxis and Migration Tool 2.0 software were used for image statistics and analysis to obtain the cell migration track and migration speed. HCC cells cultured on low-stiffness substrate were further treated with Yoda1 (an agonist for Piezo1, MedChem-Express, Shanghai, China, 25 µmol/L for MHCC97H and 5 µmol/L for Hep3B), and HCC cells cultured on high-stiffness substrate with GsMTx4 (an antagonist for Piezo1, Abcam, 2.5 µmol/L for both MHCC97H and Hep3B).

2.5. F-actin polymerization analysis of HCC cell by phalloidin staining and a confocal microscope

Wild-type, shCtrl-transfected, shITGB1-transfected and shPiezo1-transfected HCC cells were cultured on high-stiffness substrate, respectively, and they were divided into 6 groups (WT, shCtrl, shITGB1, shITGB1+Yoda1, shPiezo1, and shPiezo1+Yoda1). HCC cells in the shITGB1+Yoda1 and shPiezo1+Yoda1 groups were treated with Yoda1 (MedChemExpress, Shanghai, China, 25 µmol/L for MHCC97H and 5 µmol/L for Hep3B) for 1 h, respectively. Subsequently, the culture supernatants of HCC cells were discarded, and the cells were washed twice with PBS, each time for 5 min. Afterwards, the cells were fixed in 4 % paraformaldehyde for 15 min at room temperature, and permeabilized with 0.1 % Triton X-100 permeabilization solution for 15 min at room temperature. Finally, the cells were stained with the diluted Alexa Fluor 488 phalloidin (Invitrogen, Carlsbad, USA; 1:40 diluted with 1 % BSA) for 1 h at room temperature, and counterstained with DAPI solution (Dako, Glostrup, Denmark; 1:3000 diluted) at room temperature in dark for 5 min. F-actin polymerization was observed and analyzed by a laser confocal microscope (Zeiss LSM 800, Jena, Germany).

2.6. A matrix-gel substrate in vitro for assessing the invasion ability of HCC cells

High concentration matrigel with growth factors (Corning, New York, NY, USA), rat tail collagen I (Corning) and DMEM (or MEM) medium were mixed in a proportion of 25: 11: 14 (200 µL) and solidified to form a matrix-gel substrate (final concentration of collagen I: 2 mg/mL) in the upper chamber of Boyden chamber at 37 °C for 30 min. Approximately 2 × 10⁵ HCC cells were seeded onto the surface of the

matrix-gel substrate for short-term culture to simulate the process of HCC cells invading into ECM, and 200 µL of DMEM (or MEM) complete medium in the upper chamber, and 1 mL of the conditioned medium (fresh DMEM (or MEM): old DMEM (or MEM)) in the lower chamber were employed in this experiment. Old DMEM (or MEM) refers to the collected culture supernatant after 2 days of HCC cell culture. HCC cells seeded on the surface of the matrix gel were divided into 7 groups (cell-free, wild-type, shCtrl, shITGB1, shITGB1+Yoda1, shPiezo1, shPiezo1+Yoda1). In the shITGB1+Yoda1 and shPiezo1+Yoda1 groups, cells were treated with Yoda1 (25 µmol/L for MHCC97H and 5 µmol/L for Hep3B) during culture. After culture for 4 days, the matrix-gel substrates in each group were removed gently from the upper chamber to maintain the shape of the matrix-gel substrate, and then fixed with 4 % paraformaldehyde for 24 h, subsequently they were dehydrated as usual and vertically embedded in paraffin for tissue section and HE staining. All the procedures should be carried out gently to avoid the destroy of the matrix-gel substrate. The ability of HCC cells invading into the matrix gel was observed and analyzed under a microscope. The vertical distance from the deepest invading point to the matrix-gel surface was measured as the relative invasion distance of each group for quantification.

2.7. Western blot

Total proteins of cells and tissues were extracted using RIPA lysis buffer (Beyotime Biotechnology, Shanghai, China) containing protease/phosphates inhibitors (Beyotime Biotechnology). The protein samples from each group were equally loaded on a 10 % SDS-PAGE gel, followed by transferred to polyvinylidene difluoride (PVDF) membranes (Millipore, Schwalbach, SL, Germany) and blocked with 5 % skimmed milk. Next, the transferred PVDF membrane were probed with primary antibody, subsequently with HRP-conjugated secondary antibody (1:5000, Proteintech, Wuhan, Hubei, China), and exposed using super-sensitive electrochemiluminescence (ECL) reagents (Tanon, Shanghai, China) and the ChemiDoc XRS+Gel Imaging System (Bio-Rad, Hercules, CA, USA). The diluted primary antibodies were as follows: RhoA, ROCK1, P-MLC2(Ser19), MLC2, integrin αV, integrin α4, integrin α5, integrin α6, integrin β5, P-FAK(Tyr397), FAK, P-Src(Tyr416), Src, Arg, P-EGFR, EGFR (1:1000, Cell Signal Technology, Boston, MA, USA), Piezo1 (1:500, Abcam, Cambridge, UK), MLCK and Arg (1:1000, Proteintech, Hubei, China).

2.8. Construction of a novel subcutaneous animal model for evaluating the invasion ability of HCC

Twenty-four male BALB/c nude mice aged at 6-week-old were obtained from Shanghai SLAC Laboratory Animal Co. (Shanghai, China), and randomly divided into 8 groups on average. The hydrophilic polycarbonate filter membrane (PC membrane, 8.0 µm pore size, Millipore, Schwalbach, SL, Germany) was subjected to ethylene oxide sterilization. Small pores with a diameter of 8.0 µm in the PC membrane allowed tumor cells to pass through. Matrigel with growth factors (Corning, New York, NY, USA), rat tail collagen I (Corning) and HCC cells suspension in PBS (containing appropriate 1 × 10⁷ wild-type, shCtrl-transfected, shITGB1-transfected or shPiezo1-transfected HCC cells) were mixed in a proportion of 25: 11: 14 to form cell-embedded matrix gels (final concentration of collagen I: 2 mg/mL), and then 200 µL cell-embedded matrix gels were pipetted onto a sterile PC membrane and solidified at 37 °C for 30 min. Subsequently, the relatively uniform PC membrane packages with cell-embedded matrix gels were formed tightly sealed with surgical suture. Next, they were transplanted subcutaneously into the upper left flank region of nude mice. After 10 days, the nude mice were executed and the embedded tumor were collected. The size and wet weight of the tumor tissues were measured, and the PC filter membranes from each group were carefully obtained for Giemsa staining. Six of the magnified fields (200x) in each group were randomly

selected under a microscope for statistical analysis. All animal care and experiments used in this study were in accordance with the guideline for the Care and Use of Laboratory Animals published by the US National Academy of Science (Washington, WA, USA), and the related experiment design met with approval from the Animal Care Ethical Committee of Zhongshan Hospital, Fudan University (Shanghai, China) (Approval No. 2020-116).

2.9. The colocalization of cortactin and F-actin in HCC cells under different stiffness stimulation using double immunofluorescent staining

Wild-type HCC cells were cultured on low- and high-stiffness substrates, and a group of cells grown on high-stiffness substrate were simultaneously treated with exogenous EGF (50 ng/mL). In addition, shCtrl-transfected, shITGB1-transfected and shPiezo1-transfected HCC cells were cultured on high-stiffness substrates, and a group of shITGB1/shPiezo1-transfected HCC cells was intervened with Yoda1 (25 μmol/L for MHCC97H and 5 μmol/L for Hep3B). HCC cells grown on different stiffness substrates were fixed in 4 % paraformaldehyde at room temperature for 15 min, and then permeabilized with 0.1 % Triton X-100 permeabilization solution for 15 min at room temperature. Subsequently, they were blocked in 5 % BSA at room temperature for 1 h, and then incubated with the diluted cortactin antibody (1:1000) overnight at 4 °C. Next, the diluted Alexa Fluor 488 phalloidin (1:40) and the diluted Alexa Fluor 594 labeled goat anti mouse IgG (H + L) (1:200) were applied to react with the cells in dark for 1 h at room temperature, and ultimately DAPI solution (1:3000) used for counterstain with the cells. A laser confocal microscope was used for observation and photography. The punctate structures (yellow) formed at the colocalization of cortactin (red) and F-actin (green) represent an invadopodium. The cell nuclei are stained by DAPI (blue). All the cells in 10 visual fields in each group were recorded and the number of their punctate structures were measured. The average number of punctate structures per cell was compared and statistically analyzed.

2.10. RNA extraction and quantitative reverse transcription PCR (qRT-PCR)

Total RNA of HCC cells was extracted using Trizol reagent (Invitrogen, Carlsbad, USA). The concentration and purity of RNA were measured by NanoDrop ND-1000 (NanoDrop, Wilmington, DE, USA). Total RNA from each sample was reversely transcribed into complementary DNA (cDNA) using the Superscript First-Strand Synthesis System (Thermo Scientific, Waltham, USA). cDNA template was used for gene amplification with specific primers and qPCR SYBR Green Master Mix kit (Yeasen, Shanghai, China). The primer sequences of target genes are listed in the [Supplementary Table S1](#). Real-time quantitative PCR was conducted in QuantStudio3 (Thermo Scientific, Waltham, USA). Relative gene expression was normalized to GAPDH and reported as $2^{-\Delta Ct}$ [$\Delta Ct = Ct$ (EGF or other gene)-Ct (GAPDH)].

2.11. Immunohistochemistry (IHC)

The procedure for immunohistochemical staining was the same as the previously reported method [24]. Briefly, tissue sections were incubated with the diluted primary antibody (cortactin, 1:50, Cell Signal Technology, Boston, MA, USA; MMP14, 1:2000, Zen-Bioscience, Sichuan, China; and EGF, 1:200, Abcam, Cambridge, UK) overnight at 4 °C. Afterwards they were reacted with the corresponding HRP-conjugated secondary antibody (1:200, Affinity Biosciences, Jiangsu, China) at 37 °C for 45 min, and stained with freshly prepared DAB solution. Tissue slices were observed and photographed under a white light microscope. ImageJ software was used to calculate the grayscale values of positive tissue areas.

2.12. RhoA activation analysis

Levels of RhoA activation in HCC cells grown on high- and low-stiffness substrates were detected using Active Rho Pull-down and Detection Kit GTP loading assays (Beyotime Biotech. Inc. Shanghai). The experiment was performed according to the instruction of the kit. Briefly, Total protein of HCC cells was extracted in cell lysis buffer, and their supernatant was collected and incubated with Rhoteckin-RBD Agarose in the rotating mixer for 2 h at 4 °C. The mixture solution was centrifuged for 30 s at 6000×g and its supernatant was removed. The precipitate was washed three times using washing buffer, and then boiled in SDS-PAGE sample loading buffer, and resolved by SDS-PAGE. After membrane transferring and membrane blocking, the membrane was further incubated with RhoA rabbit monoclonal antibody and subsequently with HRP-conjugated secondary antibody. Ultimately, the membrane was exposed using ECL reagent.

2.13. Intervention of gefitinib, PP2 and SB273005

Gefitinib (EGFR inhibitor, 2 μmol/L, MCE, USA) and PP2 (Src inhibitor, 20 μmol/L, MCE, USA) was applied to treat HCC cells grown on different stiffness substrates for exploring the roles of EGFR and Src in matrix stiffness-induced invadopodia formation. Hepatic stellate cell line LX-2 cells grown on 16 kPa stiffness substrates were treated with SB273005 (integrin αV/β5 inhibitor, Selleck Chemicals, shanghai, China) at a final concentration of 0.1 μmol/L.

2.14. An HCC tissue microarray

An HCC tissue microarray, constructed previously from tumor tissues of buffalo rat HCC models with different liver stiffness backgrounds [21, 24], was applied in the study to clarify the relationship between matrix stiffness and invadopodia-associated genes expression levels.

2.15. Subcutaneous injection of HCC cells to construct xenograft tumors in nude mice

Forty-eight male BALB/c nude mice aged at 6-week-old were obtained from Shanghai SLAC Laboratory Animal Co. (Shanghai, China), and randomly divided into 8 groups on average. Matrigel with growth factors (Corning, New York, NY, USA), rat tail collagen I (Corning) and HCC cells suspension in PBS (containing appropriate 1×10^7 wild-type, shCtrl-transfected, shITGB1-transfected or shPiezo1-transfected HCC cells) were mixed in a proportion of 25: 11: 14 to form 200 μL of cell-embedded matrix gels (final concentration of collagen I: 2 mg/mL), and subcutaneously injected into the upper left flank region of nude mice. The growth of subcutaneous tumors in MHCC97H group and Hep3B group was analyzed on the 13th and 27th day after injection. The size and wet weight of the tumor tissues were measured.

2.16. Associations of PFS with clinicopathologic characteristics in HCC patients

The study was approved by the Zhongshan Hospital Research Ethics Committee (Approval No. B2020-018R). Clinical and pathological data of 68 patients who underwent curative resection at the Department of Liver Surgery, Zhongshan Hospital of Fudan University between July 2015 and August 2017 were analyzed. Patients were followed up till October 2018. HCC patients were diagnosed according to the diagnostic criteria of the American Association for the Study of Liver Diseases (2018), and their clinical stage was determined according to the Barcelona Clinic Liver Cancer staging system (2004) and the 8th edition of Tumor Node Metastasis (TNM) staging system, respectively. Tumor differentiation grade was evaluated by the Edmonson grading system. Among all the patients, those with PFS ≤ 24 months belong to the short-PFS group (42 cases), and those with PFS > 24 months belong to the

long-PFS group (26 cases). Statistical analysis was conducted on the following clinical and pathological parameters between two groups such as gender, age, liver stiffness, tumor size, tumor capsule integrity, microvascular invasion (MVI), tumor differentiation (Edmondson Steiner grade), Metavir's G grade, Metavir's S grade, AFP, total bilirubin TB, conjugated bilirubin CB, ALB, ALP, GGT, ALT, AST, APTT, PT, blood glucose.

2.17. The cancer genome atlas (TCGA) database

Clinical data of 372 HCC patients and the results of their tumor gene expression were downloaded from TCGA database (<https://www.cancer.gov/tcg>) on September 9, 2019 (Version: v18.0). Referring to the reported methods from our research group [23], 119 HCC patients with COL1A1^{High}/LOX^{High} were enrolled as the high stiffness group, and 120 with COL1A1^{Low}/LOX^{Low} as the low stiffness group. Survival analysis was conducted on high and low stiffness groups. Further analyses of the TCGA-LIHC cohort were made using the single gene survival analysis function of the GEPIA website. The mRNA expression levels of cortactin, MMP14, and EGF between the two groups were comparatively analyzed.

2.18. Statistical analysis

Statistical analysis was performed by SPSS version 20 software (SPSS Inc., Chicago, IL, USA) and GraphPad Prism 8.0 (GraphPad Software, La Jolla, CA, USA). Continuous variables are represented by mean \pm standard deviation. Categorical variables were analyzed by Pearson's chi-squared test. Statistical comparisons between only two groups were carried out by Student's t-test. One-way ANOVA was used for multiple-group comparisons. Kaplan Meier method (log rank test) was used for Survival analysis. $P < 0.05$ indicates statistical significance.

3. Results

3.1. Increased matrix stiffness significantly enhances migration and invasion abilities of HCC cells

Considering that high motility and invasion abilities can indirectly reflect invadopodia formation of cancer cells, we first evaluated the effects of increased matrix stiffness on the motility and invasion phenotypes of HCC cells. We prepared three stiffness substrates of 6 kPa (L), 10 kPa (M), and 16 kPa (H) as described previously [28] to mirror tissue stiffness of normal liver, fibrotic liver and cirrhotic liver, respectively [28], and conducted a real-time migration analysis of HCC cells cultured on three stiffness substrates (L, M, H). The results demonstrated that increased matrix stiffness significantly improved the migration range and speed of HCC cells, suggesting that the migration ability of HCC cells is obviously enhanced with the increase of matrix stiffness (Fig. 1A and B). Simultaneously, downregulation of integrin $\beta 1$ or Piezo1 (Figs. S1A–E), identified as the mechanosensor in our previous studies [23,24], evidently attenuated the migration range and speed of HCC cells grown on high-stiffness substrate (Fig. 1A and B), further validating the promoting effect of matrix stiffness on migration phenotype of HCC cells. Due to a positive correlation described previously between the expression level of Piezo1 and its activation level in HCC cells under different stiffness stimulation [23], we continued to apply Yoda1 (Piezo1 agonist) and GsMTx4 (Piezo1 antagonist) to treat HCC cells cultured on low- and high-stiffness substrate respectively, and found that Piezo1 activation or inhibition effectively reversed the migration range and speed of HCC cells induced by low- or high-stiffness stimulation (Fig. 1A and B), meaning that Piezo1 activation, like its expression, also mediated matrix stiffness-promoted cell migration. F-actin polymerization level is often used to indicate the ability of cell motility [3]. The results of phalloidin staining revealed that suppression of integrin $\beta 1$ or Piezo1 altered the morphology and F-actin polymerization of HCC cell grown on high-stiffness substrate significantly, whereas

Yoda1 intervention partially abrogated the changes of shITGB1 or shPiezo1-caused morphology and F-actin polymerization (Fig. 1C; Fig. S1F), in accordance with the results of cell migration. The above phenomenon all supported that increased matrix stiffness significantly enhanced the migration ability of HCC cells via integrin $\beta 1$ and Piezo1.

We developed two new experiment systems *in vitro* and *in vivo* to further clarify the effect of matrix stiffness on the invasion ability of HCC cells. We prepared a matrix-gel substrate *in vitro* by mixing Matrigel, collagen I, and DMEM/or MEM medium in a proportion of 25: 11: 14 and seeded HCC cells onto the surface of the matrix gel for short-term culture, which simulated the process of HCC cells invading into the matrix gel. Since Matrigel-contained cytokines such as EGF being able to induce invadopodia formation [41], the ability of HCC cells invading into the matrix-gel substrate represented the formation of invadopodia in this experiment system. Compared with that of non-cell group, the surface of the matrix-gel substrate of HCC-WT group and HCC-shCtrl group all displayed obviously deep invaded-depth (Fig. 1D; Fig. S1G), implying that HCC cells grown on the matrix-gel substrate have a strong invasion ability, however, the surface of the matrix-gel substrate of HCC-shITGB1 group and HCC-shPiezo1 group exhibited relatively shallow invaded-depth, moreover Yoda1 intervention reversed the invasion phenotype of HCC cells with shITGB1 or shPiezo1 and caused the reappearance of deep invaded-depth (Fig. 1D; Fig. S1G). These results suggested that downregulation of mechanosensor (integrin $\beta 1$ or Piezo1) attenuated matrix stiffness-strengthened invasion ability in HCC cells. To verify the above phenomena *in vivo*, we developed a novel subcutaneous animal model for testing the invasion ability of HCC cells *in vivo*. HCC cells (wild-type, shCtrl-transfected, shITGB1-transfected and shPiezo1-transfected HCC cells) suspended in Matrigel and collagen I were solidified and wrapped with a sterilized filter membrane to form the uniform filter membrane packages with cell-embedded matrix gels, and then transplanted subcutaneously into the upper left flank region of nude mice (Fig. S2A). The filter membrane has small pores with a diameter of 8.0 μm which allows tumor cells to pass through. Ten days later, the embedded tumors and their filter membranes were collected. The weight and volume of tumors in the packages from shITGB1 and shPiezo1-transfected MHCC97H cells were slightly decreased compared with that from WT and shCtrl-transfected MHCC97H, but there were no significant differences in the weight and volume of tumors from Hep3B cells among four groups (Figs. S2B–C). However, the number of the cells on filter membrane in shITGB1 and shPiezo1 groups were all significantly decreased (Fig. 1E and F; Fig. S2A), indicating that inhibition of mechanosensor causes an obviously decrease in the invasion ability of HCC cells. Based on the above evidence, we concluded that increased matrix stiffness significantly enhances migration and invasion abilities of HCC cells via integrin $\beta 1$ and Piezo1, indirectly suggesting the promoting effect of matrix stiffness on the formation of invadopodia.

3.2. Increased matrix stiffness obviously promotes the formation of invadopodia in HCC cells

In addition to the above indirect evidence, we further searched for the direct evidence of increased matrix stiffness regulating invadopodia formation. Colocalization expression analysis of cortactin and F-actin in cancer cells was frequently employed to determine the number of invadopodia [3,9,42]. We first comparatively analyzed the colocalization expressions of cortactin and F-actin in HCC cells under high- and low-stiffness stimulation, and discovered that the number of invadopodia (yellow punctate structure) in HCC cell grown on high-stiffness substrate was significantly higher than that in HCC cells grown on low-stiffness substrate (Fig. 2A and B), and EGF intervention further increased the number of invadopodia in HCC cells grown on high-stiffness substrate (Fig. 2A and B), illuminating that high-stiffness stimulation not only directly promotes invadopodia formation, but also synergistically enhance this effect with exogenous EGF.

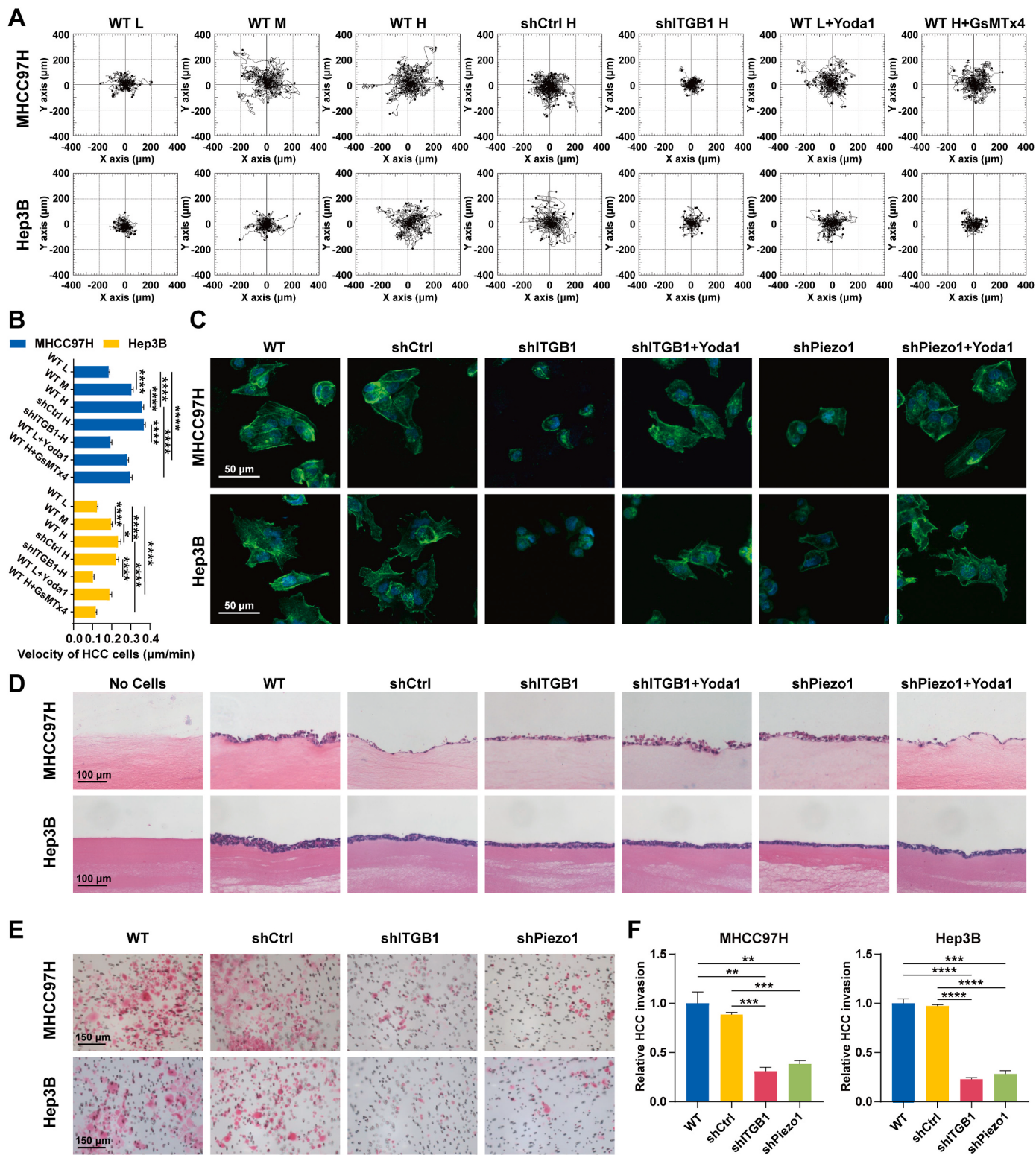


Fig. 1. Increased matrix stiffness significantly enhances migration and invasion abilities of HCC cells. (A) A real-time analysis of cell migration under different stiffness stimulation using a Cell IQ living cell workstation. In the right two panels, HCC cells grown on low-stiffness substrate were treated with Yoda1 (25 μmol/L for MHCC97H and 5 μmol/L for Hep3B), and HCC cells on high-stiffness substrate were treated with GsMTx4 (2.5 μmol/L for both MHCC97H and Hep3B). (B) Quantification of velocity of HCC cells (μm/min) shown in (A). A total of 40 cells were randomly selected in each group for statistical analysis. (C) F-actin polymerization analysis of HCC cells grown on high-stiffness substrate using phalloidin staining. Scale bar: 50 μm. (D) Assessing the invasion ability of HCC cells and HCC cells with integrin β1 and Piezo1 knockdown using a matrix-gel substrate *in vitro*. Scale bar: 100 μm. (E, F) A novel subcutaneous tumor nude mouse model established for evaluating the invasion ability of HCC. The numbers of invaded cells on filter membrane in HCC-shITGB1 and HCC-shPiezo1 groups were significantly lower than those in HCC-WT and HCC-shCtrl groups. Scale bar: 150 μm. Data are representative images and expressed as mean ± SD of each group from three separate experiments. *P < 0.05, **P < 0.01, ***P < 0.001, ****P < 0.0001. H: High. L: Low.

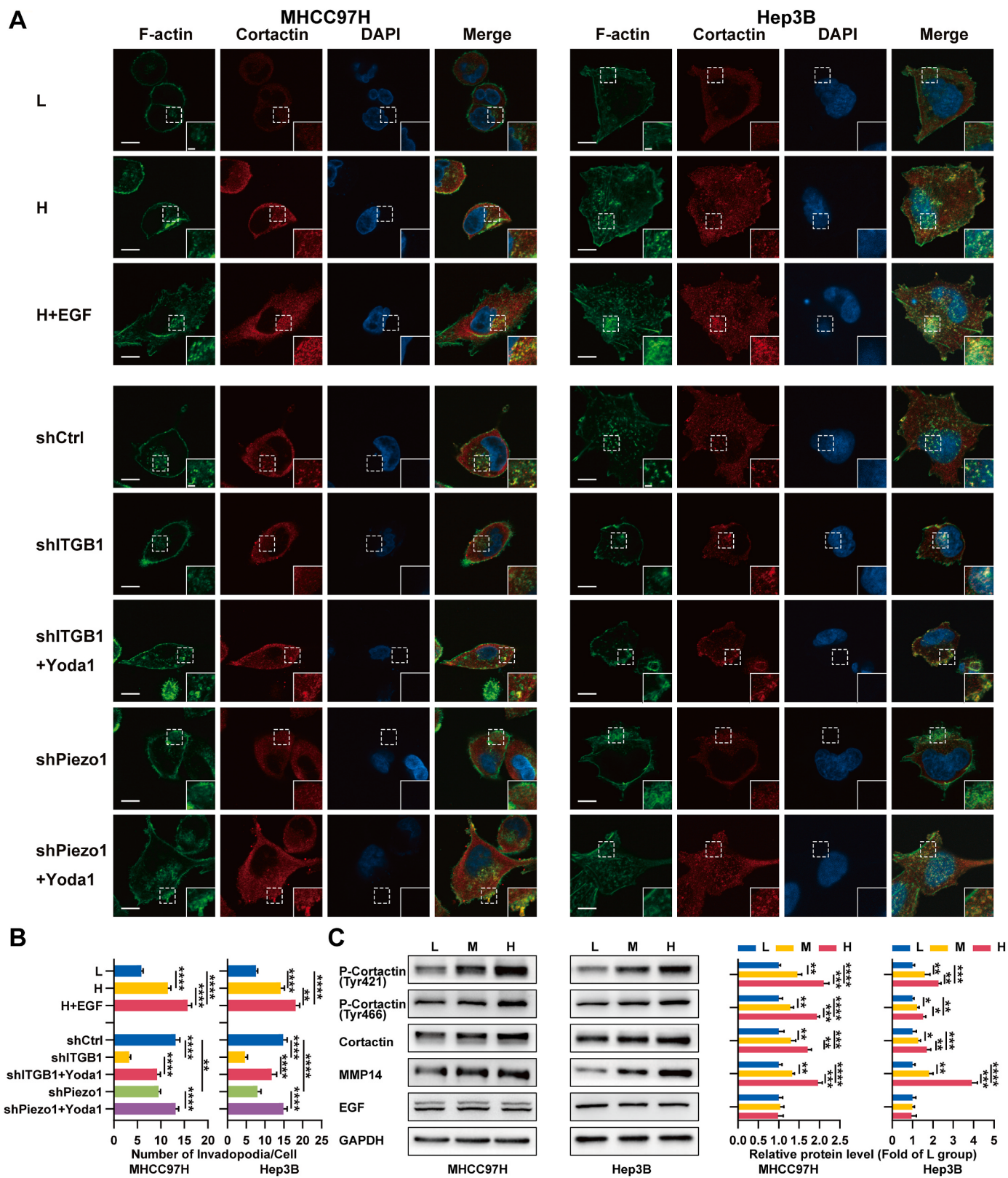


Fig. 2. Increased matrix stiffness obviously promotes the formation of invadopodia in HCC cells. (A) Colocalization expression of F-actin and cortactin in HCC cells under different stiffness stimulation and exogenous EGF stimulation (the upper three line panels). The bottom five line panels showed colocalization expression of F-actin and cortactin in shCtrl-transfected, shITGB1-transfected and shPiezo1-transfected HCC cells cultured on high-stiffness substrates, and a group of shITGB1 or shPiezo1-transfected HCC cells intervened with Yoda1 (25 μ mol/L for MHCC97H and 5 μ mol/L for Hep3B). Insets depict magnification of boxed areas showing invadopodia. Scale bars: (main images) 10 μ m; (insets) 2 μ m. (B) Quantification of the numbers of invadopodia per cell in (A). (C) The expression levels of invadopodia-associated proteins and EGF in HCC cells grown on different stiffness substrates. Data are representative images and expressed as mean \pm SD of each group from three separate experiments. *P < 0.05, **P < 0.01, ***P < 0.001, ****P < 0.0001. H: High. M: Medium. L: Low.

Subsequently, we further examine whether integrin $\beta 1$ and Piezo1 mediated matrix stiffness-induced invadopodia formation. The results revealed that suppression of integrin $\beta 1$ or Piezo1 remarkably reduced the number of invadopodia in HCC cells cultured on high-stiffness substrate, and Yoda1 intervention abrogated this effect and increased the number of invadopodia, indicating that Piezo1 activation can partially counteract the effect of integrin $\beta 1$ or Piezo1 suppression on the formation of invadopodia induced by high stiffness (Fig. 2A and B). Besides, we comparatively analyzed the expression levels of invadopodia-associated genes in HCC cells under different stiffness stimulation and found that increased matrix stiffness evidently upregulated the expressions of invadopodia-associated proteins/genes (cortactin and MMP14), as well as the phosphorylation level of cortactin (Tyr421 and Tyr466), but little effect on EGF expression (Fig. 2C; Figs. S3A and B). Using an HCC tissue microarray prepared previously from buffalo rat HCC models with different liver stiffness backgrounds [21,24], we also found that the expression levels of invadopodia-associated proteins and EGF were all enhanced with increase of liver stiffness backgrounds (Fig. 3A). Additionally, we developed subcutaneous tumor nude mouse models by injecting the suspended HCC cells in the mixture of Matrigel and collagen I to assess the effect of integrin $\beta 1$ and Piezo1 knockdown on matrix stiffness-induced invadopodia formation. The results demonstrated that the weight and volume of subcutaneous tumors in HCC-shITGB1 and HCC-shPiezo1 groups were all decreased compared with that in HCC-WT and HCC-shCtrl groups (Fig. 3B). Simultaneously, the expression levels of cortactin, MMP14 and EGF in HCC-shITGB1 and HCC-shPiezo1 groups were also significantly decreased (Fig. 3C; Fig. S4A), further confirming that downregulation of mechanosensor apparently suppresses the expressions of invadopodia-associated genes. Taken together, the changes described above in cell invasive phenotypes, the number of invadopodia and invadopodia-associated genes expression all support that a close linkage exists between matrix stiffness and invadopodia formation in HCC cells, and increased matrix stiffness obviously promotes the formation of invadopodia. Interestingly, an obvious overexpression in EGF at the tissue level was found with the increase of matrix stiffness (Fig. 3A), but no significant change at the cell level (Figs. S3A and B; Fig. 2C), implying that EGF overexpression at the tissue level may mainly due to the secretion of non-cancer cells within microenvironment.

3.3. Increased matrix stiffness activates RhoA/ROCK1 and MLCK pathways to accelerate the migration of HCC cells

Increased matrix stiffness regulates cell migration by remodeling cytoskeleton structure [38]. Myosin II as an important cytoskeleton protein affects cytoskeleton contraction and cell migration [15], and phosphorylation level of myosin light chain (MLC) often reflect the activity of myosin II. Rho kinase (ROCK) and myosin light chain kinase (MLCK) are all able to increase the phosphorylation level of MLC [16]. Additionally, MLCK activity is calcium ion dependent [43]. Our recent work demonstrates that Piezo1, a mechanosensitive ion channel protein, can sense stiffness mechanical signal to increase the influx of calcium ions in HCC cells [23]. Hereby, it is supposed that the activation of ROCK and MLCK may activate MLC together to participate in matrix stiffness-induced cell migration. We analyzed the activation state of RhoA/ROCK1 and MLCK pathways in HCC cells grown on different stiffness substrates, and found that the expression levels of RhoA, Rock1, MLCK, the phosphorylation level of MLC2 (Ser19) and the activation level of RhoA were all increased significantly with the increase of matrix stiffness (Fig. 4A; Fig. S4B). Suppression of integrin $\beta 1$ obviously downregulated the expression of RhoA and ROCK1 and the phosphorylation level of MLC2 (Ser19) in HCC cells grown on high-stiffness substrate (Fig. 4B), suggesting that weakening mechanotransduction partially attenuates the activity of Rho/ROCK1 pathway. On the other hand, we applied GsMTx4 to treat HCC cells cultured on high-stiffness

substrate and found that the intervention of GsMTx4 could significantly decrease the expression of MLCK and the phosphorylation level of MLC2 (Ser19) (Fig. 4C). In contrast, using Yoda1 to treat HCC cells cultured on low-stiffness substrate, the expression of MLCK and the phosphorylation level of MLC2 (Ser19) were remarkably upregulated (Fig. 4D), validating that Piezo1 activation regulates MLC2 phosphorylation through MLCK. The above results suggest that increased matrix stiffness not only activates RhoA/ROCK1 pathway through integrin $\beta 1$, but also stimulate Piezo1 activity to increase calcium ion influx and MLCK activity. These two pathways jointly increased MLC2 phosphorylation to activate myosin II and promoted cytoskeleton remodeling and cell migration (Fig. 4E).

3.4. Direct and indirect regulatory pathways synergistically participate in matrix stiffness-driven invadopodia formation in HCC cells

EGF is a strong inducer for invadopodia formation [41]. Activated HSCs not only secrete a variety of cytokines including EGF [44], but also contributes to matrix stiffening and HCC progression [39]. Importantly, high-stiffness signal can stimulate the sustained activation of HSCs [40], and the results in Fig. 3A, Fig. S3 and Fig. 2C revealed an obvious overexpression in EGF at the tissue level but no significant change at the cell level, we therefore conjectured that high expression of EGF at the tissue level is likely come from HSCs secretion, and biomechanical signal and paracrine-produced EGF may synergistically participate in matrix stiffness-driven invadopodia formation. We first evaluated the effect of increased matrix stiffness on EGF expression in HSCs, and found that the expression of EGF in HSCs grown on high-stiffness substrate was remarkably higher than that in HSCs grown on low-stiffness substrate (Fig. 5A), suggesting that increased matrix stiffness indeed upregulates EGF expression in HSCs. Subsequently, we analyzed the differential expressions of integrin subtypes in HSCs grown on different stiffness substrates, and discovered that integrin αV and integrin $\beta 5$ expressions were all noticeably enhanced in HSCs with increase of matrix stiffness, but little change in other integrin subtypes (Fig. 5B), indicating that integrin $\alpha V/\beta 5$ may mediate stiffness signal into HSCs. Because activation of PI3K/Akt signaling pathway was reported to influence EGF expression [39], we continued to clarify whether stiffness mechanical signal upregulated EGF expression in HSCs via activating integrin $\alpha V\beta 5/PI3K/Akt$ pathway. The results demonstrated that the expressions of PI3K, EGF and the phosphorylation level of Akt in HSCs grown on high-stiffness substrate were all obviously higher than those in HSCs grown on low-stiffness substrate (Fig. 5C), meaning that increased matrix can activate PI3K/Akt signaling pathway and upregulate EGF expression in HSC cells. Meanwhile, integrin $\alpha V/\beta 5$ inhibitor SB273005 could partially reverse the activation of PI3K/Akt pathway and the expression of EGF in HSC cells under high stiffness stimulation (Fig. 5C), verifying that integrin $\alpha V/\beta 5$ mediates stiffness signal into HSCs to activate this signal pathway. So, it is easy to determine that increased matrix stiffness upregulates EGF expression in HSCs by activating integrin $\alpha V\beta 5/PI3K/Akt$ pathway. Combining the results of Fig. 2 that high-stiffness stimulation and exogenous EGF could synergistically increase the number of invadopodia in HCC cells, a synergistic regulation may exist between high-stiffness stimulation and paracrine-produced EGF in the formation of invadopodia.

We further explored how biomechanical signal and paracrine-produced EGF synergistically regulate matrix stiffness-driven invadopodia formation. Activation of EGFR/Src/Arg/cortactin pathway has been documented to participate in EGF-induced invadopodia formation in breast cancer cells [45]. We firstly examined whether this pathway also works in matrix stiffness-driven invasopodia formation in HCC cells. Compared with that in the control cells grown on low-stiffness substrate, the phosphorylation levels of FAK, Src, cortactin (tyr421 and tyr466) and the expressions of Arg, MMP14 in HCC cells grown on high-stiffness substrate were all significantly increased (Fig. 6A; Fig. S5A), suggesting that high stiffness signal activate

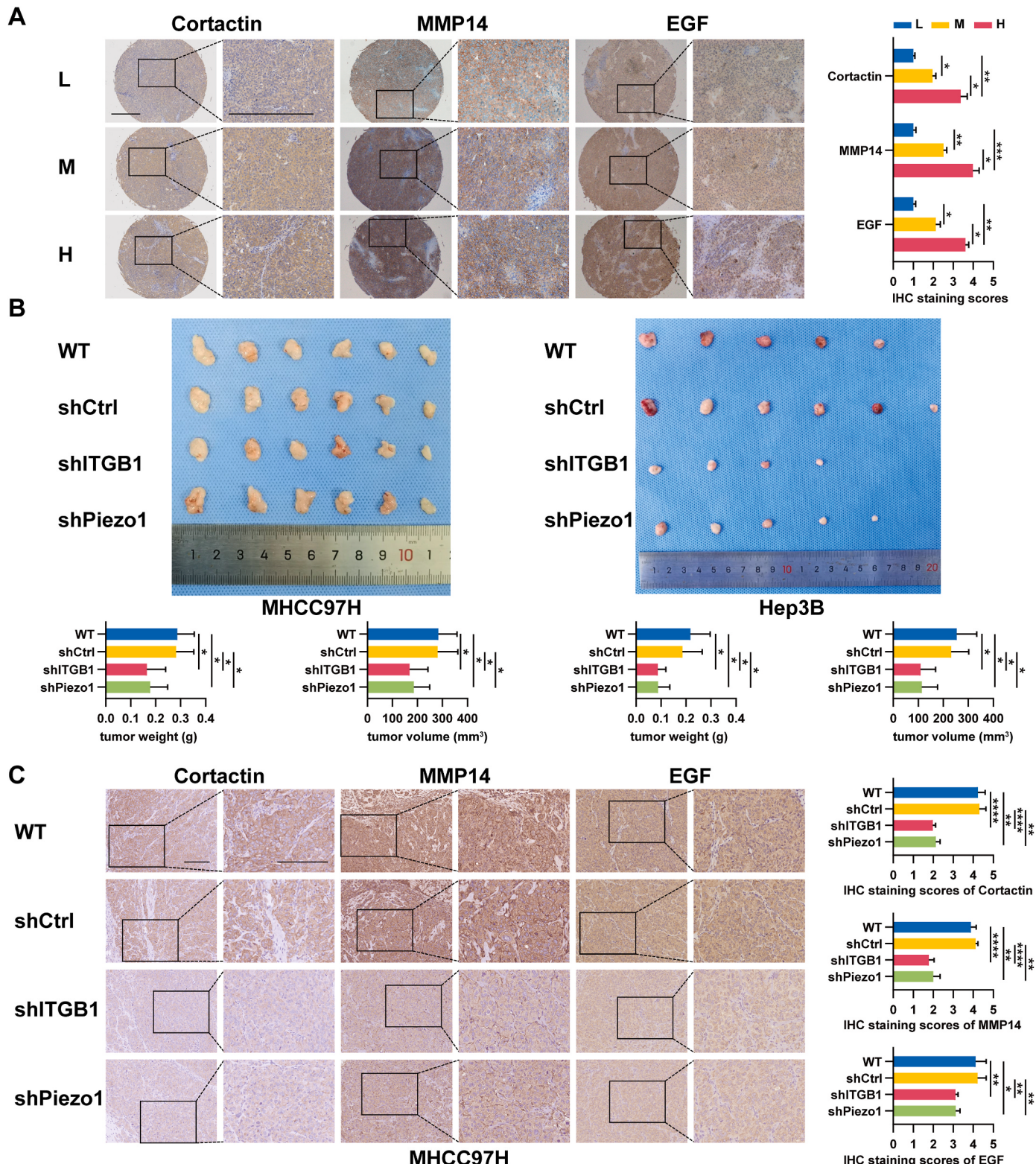


Fig. 3. Validation of tissue expression levels of invadopodia-associated proteins and EGF. (A) The expression analysis of invadopodia-associated proteins and EGF in an HCC tissue microarray prepared previously from buffalo rat HCC models with different liver stiffness backgrounds. Scale bars: 500 μm . (B) The weight and volume analysis of subcutaneous tumor nude mouse models developed by injecting the suspended HCC cells in the mixture of Matrigel and collagen I. (C) Tissue expression levels of invadopodia-associated proteins and EGF under integrin $\beta 1$ or Piezo1 knockdown. Scale bars: 150 μm . Data are representative images and expressed as mean \pm SD of each group from three separate experiments. * $P < 0.05$, ** $P < 0.01$, *** $P < 0.001$, **** $P < 0.0001$.

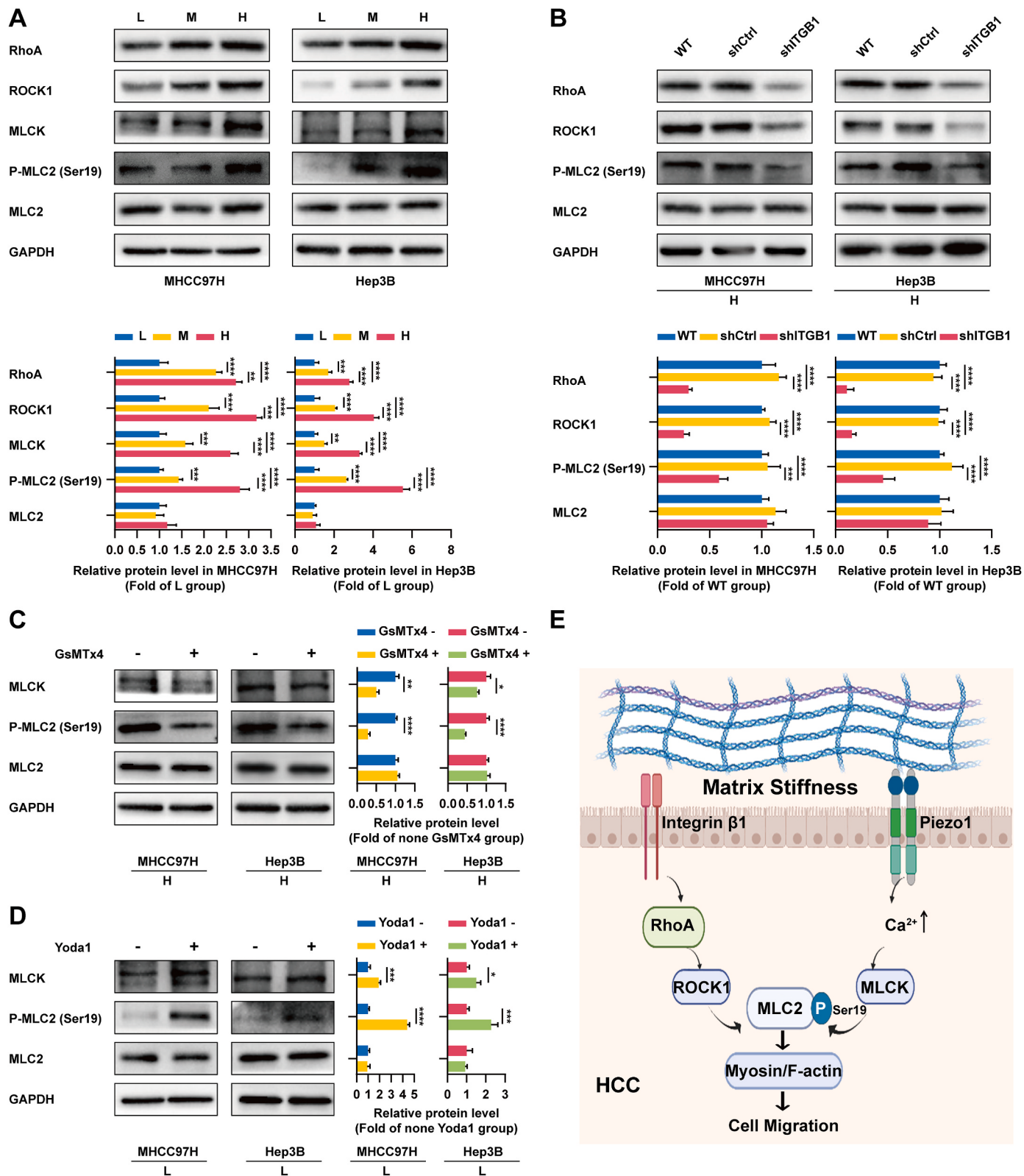
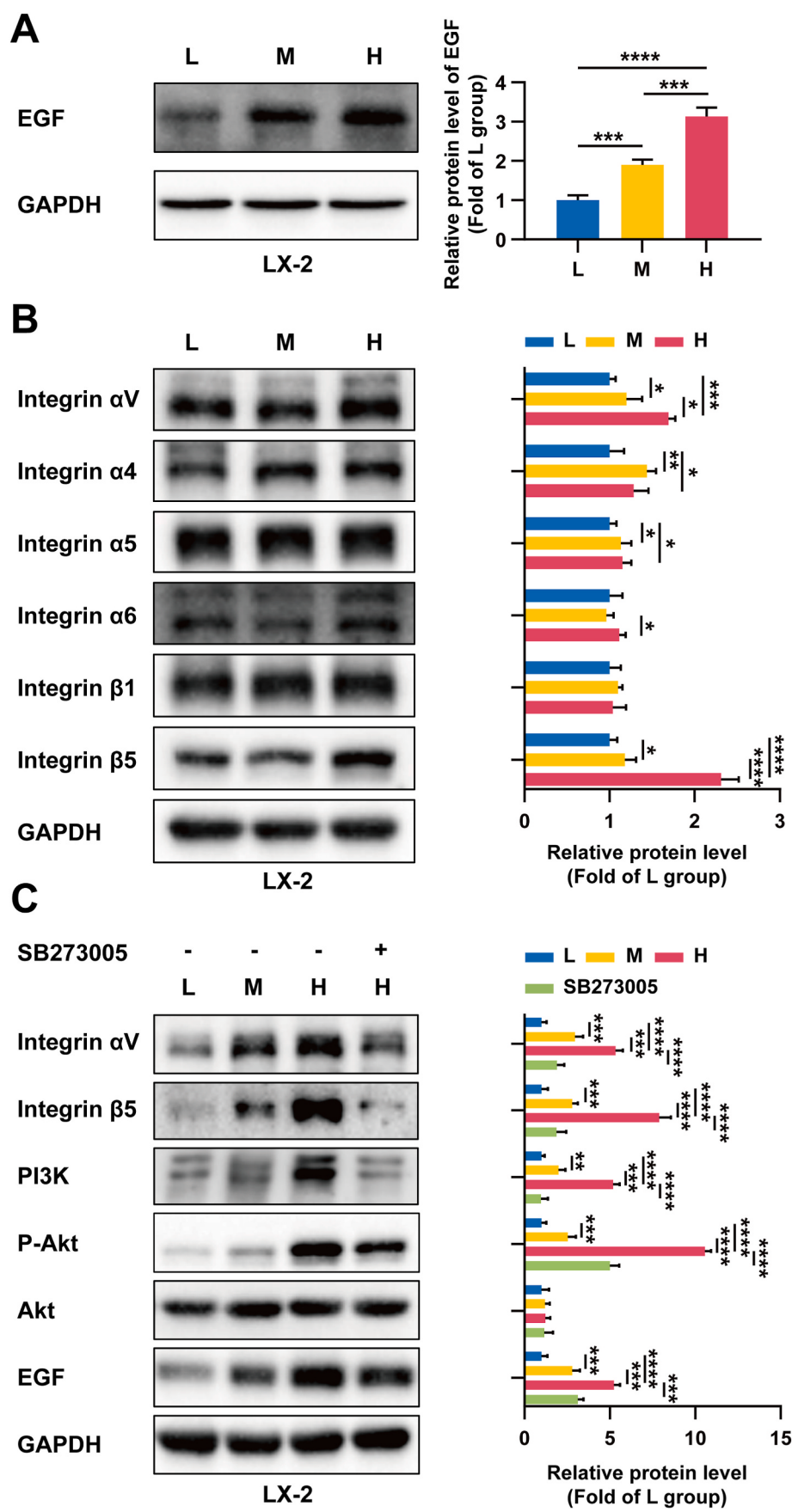


Fig. 4. Activation of RhoA/ROCK1 and MLCK pathways are involved in matrix stiffness-accelerated cell migration. (A) Comparative analysis of the activation state of RhoA/ROCK1 and MLCK pathways in HCC cells grown on different stiffness substrates. (B) The effects of integrin $\beta 1$ knockdown on the expression of RhoA and ROCK1 and the phosphorylation of MLC2 (Ser19). (C, D) The inactivity and activity of Piezo1 channel obviously affected MLCK/MLC2 pathway in HCC cells grown on low- and high-stiffness substrate. (E) The underlying mechanism of matrix stiffness-accelerated cell migration. Data are representative images and expressed as mean \pm SD of each group from three separate experiments. * $P < 0.05$, ** $P < 0.01$, *** $P < 0.001$, **** $P < 0.0001$.



(caption on next page)

Fig. 5. Increased matrix stiffness significantly upregulated EGF expression in hepatic stellate cells (HSCs). (A) The effect of increased matrix stiffness on the expression of EGF in HSCs. (B) Differential expression analysis of integrin subtypes in HSCs grown on different stiffness substrates. (C) Increased matrix stiffness activated integrin $\alpha V\beta 5/PI3K/Akt$ pathway to upregulate EGF expression in HSCs. Data are representative images and expressed as mean \pm SD of each group from three separate experiments. * $P < 0.05$, ** $P < 0.01$, *** $P < 0.001$, **** $P < 0.0001$.

FAK/Src/Arg/cortactin pathway. Simultaneously, stimulation of exogenous EGF led to a more significant increase in the expression of these signaling molecules mentioned above except for phosphorylation of FAK (Fig. 6A; Fig. S5A). Subsequently, we applied a combination of EGF and EGFR inhibitor (gefitinib) to treat HCC cells grown on high-stiffness substrate, and found that the phosphorylation of EGFR, Src, cortactin (tyr421 and tyr466) and the expression of Arg, MMP14 were all significantly decreased except for the phosphorylation of FAK (Fig. 6B; Fig. S5B). As cortactin phosphorylation and MMP14 were two marker molecules of invadopodia, the above results supported that there was a synergistic promoting effect between high-stiffness stimulation and EGF in invadopodia formation. Src/Arg/cortactin pathway was a common downstream pathway of matrix stiffness and EGF, but the phosphorylation level of their upstream FAK was only in response to stiffness mechanical stimulation rather than EGF stimulation. Then, we further testified that matrix stiffness itself was able to activate Src/Arg/cortactin pathway independently. Suppression of integrin $\beta 1$ and Piezo1 all obviously attenuated the phosphorylation levels of FAK, Src, cortactin and the expressions of Arg and MMP14 in HCC cells grown on high-stiffness substrate, indicating that high stiffness signal indeed activated Src/Arg/cortactin pathway independently through integrin $\beta 1$ and Piezo1 (Fig. 6C and D; Figs. S5C and D). Additionally, GsMTx4 intervention could significantly inhibit the activation of FAK/Src/Arg/cortactin pathway and the expression of MMP14 in HCC cells grown on high-stiffness substrate (Fig. 6E; Fig. S5E). On the contrary, Yoda1 intervention could promote the activation of FAK/Src/Arg/cortactin pathway and the expression of MMP14 in HCC cells grown on low-stiffness substrate (Fig. 6E; Fig. S5E). In combination with the above experimental results that EGF stimulation significantly improved the phosphorylation of Src, cortactin and the expressions of Arg and MMP14, but had little effect on the phosphorylation level of FAK, we ascertained that Src was the common hub molecule of two regulatory pathways of matrix stiffness and EGF. We further used EGF alone and a combination of EGF and Src inhibitor (PP2) to separately treat HCC cells cultured on high-stiffness substrate, and discovered that the phosphorylation levels of Src, cortactin and the expression of Arg, MMP14 were all significantly decreased in the combination intervention group, but no significant changes in the phosphorylation levels of EGFR and FAK (Fig. 6F; Fig. S5F), confirming that Src was the common hub molecule of matrix stiffness and EGF regulatory pathways. Together, two regulatory pathways synergistically participated in matrix stiffness-driven invadopodia formation, including directly inducing invadopodia formation of HCC cells via activating integrin $\beta 1$ or Piezo1/FAK/Src/Arg/cortactin pathway, and indirectly stimulating invadopodia formation through improving EGF production to activate EGFR/Src/Arg/cortactin pathway.

3.5. Correlation between matrix stiffness and invadopodia-associated genes and its clinical significance

The expression levels of COL1 and LOX can better indicate the level of liver matrix stiffness [23]. Taking the median expression value of COL1 and LOX in TCGA-HCC tissue as the threshold, we divided TCGA-HCC patients into the high-stiffness group (120 cases) and the low-stiffness group (119 cases) to testify the relationship between matrix stiffness and invadopodia-associated genes. The results showed that the expression levels of cortactin, MMP14 and EGF in the high-stiffness group were obviously higher than those in the low-stiffness group (Fig. S6A), and the overall survival time of HCC patients in the high-stiffness group was significantly shorter than that in low-stiffness

group ($P < 0.05$) (Fig. 7A), suggesting that matrix stiffness is positively correlated with the expression levels of invadopodia-associated genes, and high matrix stiffness indicates unfavorable prognosis. In addition, compared with those with low expression of cortactin, HCC patients with high expression of cortactin had significantly shorter overall survival time. Similarly, HCC patients with high expression of MMP14 or EGF also exhibited shorter overall survival time (Fig. 7B), demonstrating that high expressions of invadopodia-associated genes also indicate worse prognosis of HCC patients. Subsequently, we retrospectively analyzed the clinicopathological data of HCC patients who underwent surgical resection in Zhongshan Hospital Affiliated to Fudan University from July 2015 to August 2017. According to a cutoff value of PFS ≤ 24 months, the patients were classified into short PFS group (42 cases) and long PFS group (26 cases). The results demonstrated that shorter PFS was significantly associated with liver stiffness, microvascular invasion, tumor differentiation, Metavir's S score, AFP and APTT (Table 1), meaning that the above indicators may be the influencing factors of short PFS (Table 1). It can be inferred that high liver stiffness may promote the progression of HCC and cause poor prognosis, in accordance with our previous findings [21,23,26–28]. Additionally, we used 8 HCC tissues from each of the long- and short-PFS groups to detect the expressions of invadopodia-associated proteins. Compared with those in the long-PFS group, the expressions of integrin $\beta 1$, Piezo1, EGF, cortactin, MMP14 and the phosphorylation level of cortactin (tyr421 and tyr466) in the short-PFS group were all upregulated, further validating a positive correlation among PFS, matrix stiffness and invadopodia-associated proteins (Fig. 7C). These clinical data suggested the role of increased matrix stiffness in promoting invadopodia formation and HCC progression.

4. Discussion

Metastasis is the leading cause of cancer-related death and a major clinical challenge for improving therapeutic effect and prognosis of cancer. Cancer metastasis is generally inseparable from the formation of invadopodia, and the ability to form invadopodia often reflect the malignancy degree of cancer cells. So, exploring the regulatory mechanism of invadopodia formation is undoubtedly an ideal shortcut to better understand metastasis and discover new targets for cancer intervention. Invadopodia can exert great impact on degrading extracellular matrix (ECM) and promoting local invasion, intravasation and extravasation process during metastasis [8–11], thus its formation often serves as a key molecular event to determine the rate and route of metastatic dissemination [2,5]. During the last two decades, the effect of biochemical stimuli on invadopodia formation and their relevant mechanism have been extensively studied. Some classic signal pathways such as PI3K/Rho/Rac/Cdc42, WASP family protein/Arp2/3 complex, LIM kinase/cofilin, cortactin, and other pathways such as ROS signaling, integrin signaling, microRNA, etc. have proposed to mediate biochemical stimuli-induced invadopodia formation [6,10,13,14,42,46,47]. However, the role of biomechanical stimuli in invadopodia formation of cancer cells, especially in HCC cells, is still largely undefined. Increased matrix stiffness is a malignant biomechanical hallmark of HCC, and accumulating evidence suggests that increased matrix stiffness remarkably strengthens the malignant characteristics of HCC cells and promotes their invasion and metastasis [18,21–36]. A study shows that HCC cells overexpress and secrete Agrin to promote the formation of Arp2/3 complex-dependent invadopodia in HCC [37], and further mechanism analysis shows that increased matrix stiffness promotes Agrin expression, and Agrin activates transcription factor YAP through the

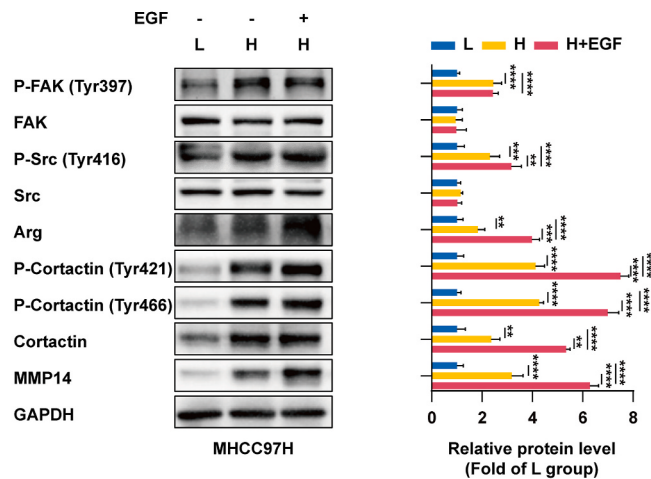
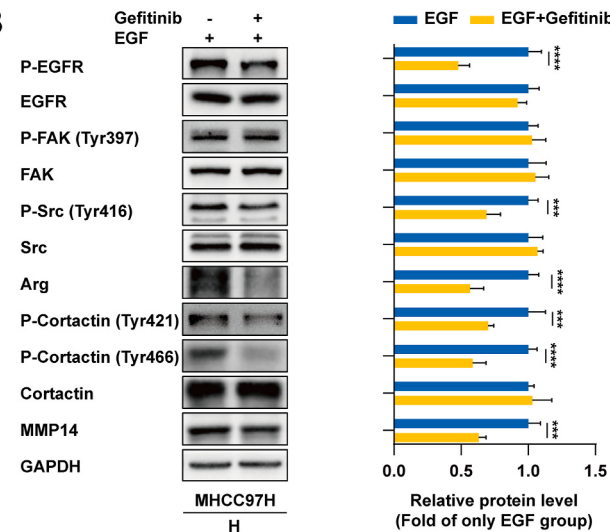
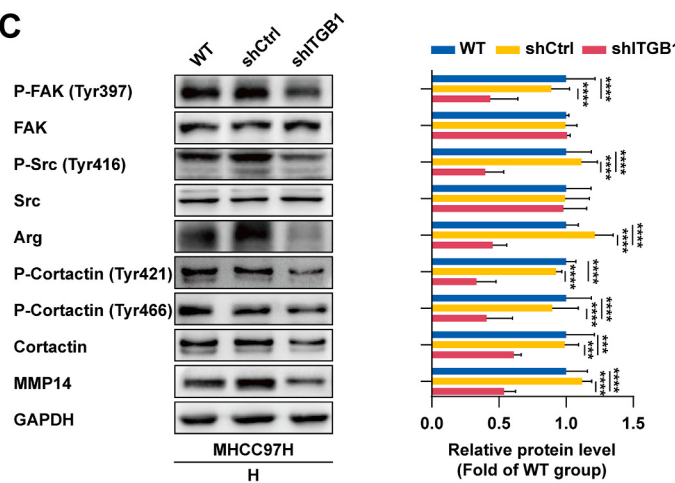
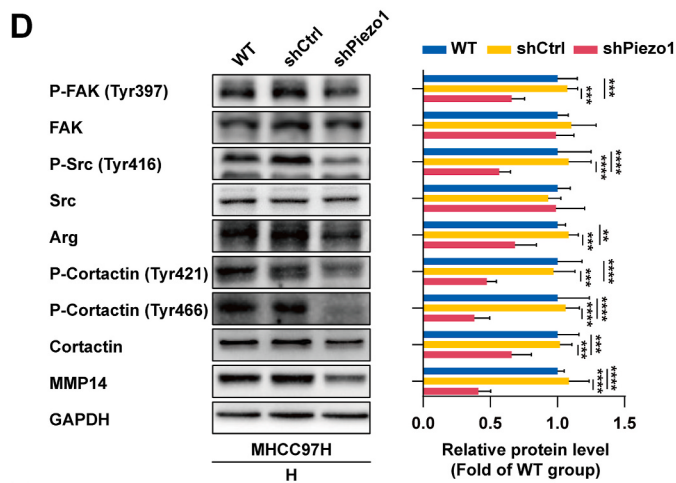
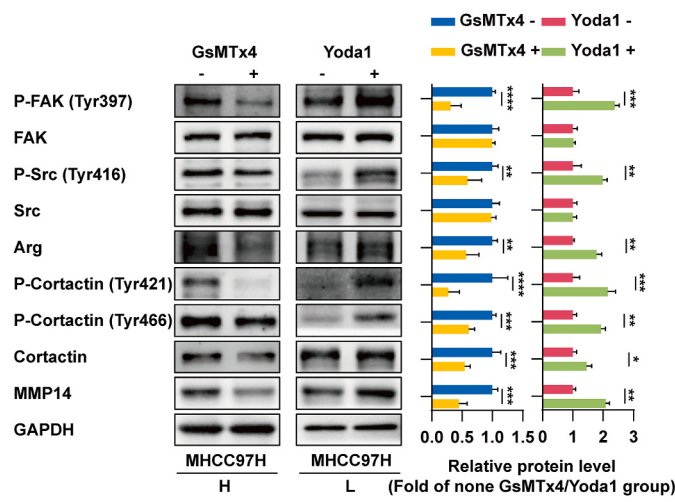
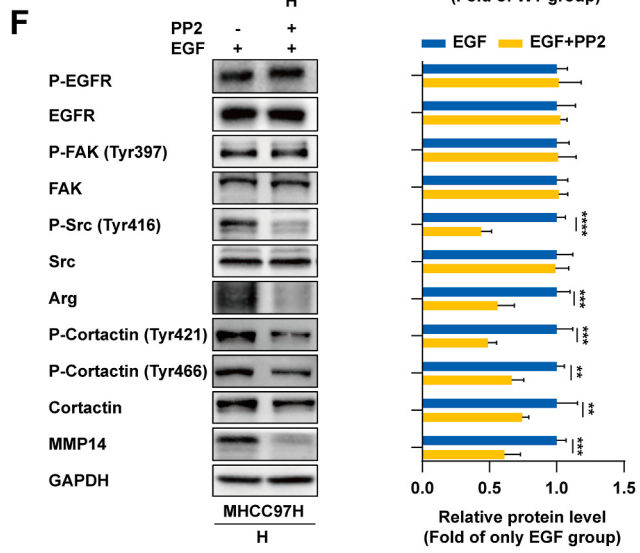
A**B****C****D****E****F**

Fig. 6. A synergistic regulation of high-stiffness stimulation and paracrine-produced EGF in the formation of invadopodia in HCC cells. (A) High stiffness stimulation obviously increased the phosphorylation levels of FAK, Src, cortactin and the expressions of Arg, MMP14 in HCC cells, and stimulation of exogenous EGF resulted in a more significant increase in the expression of the above signaling molecules except for phosphorylation of FAK. (B) Intervention of EGF and EGFR inhibitor (gefitinib) showed that except for the phosphorylation of FAK, the phosphorylation of EGFR, Src, cortactin and the expression of Arg, MMP14 were all significantly decreased in HCC cells grown on high-stiffness substrate. (C, D) Suppression of integrin $\beta 1$ or Piezo1 obviously attenuated the phosphorylation levels of FAK, Src, cortactin and the expressions of Arg, and MMP14 in HCC cells grown on high-stiffness substrate. (E) GsMTx4 intervention significantly inhibited the activation of FAK/Src/Arg/cortactin pathway and the expression of MMP14 in HCC cells grown on high-stiffness substrate, while Yoda1 intervention obviously promoted the activation of FAK/Src/Arg/cortactin pathway and the expression of MMP14 in HCC cells grown on low-stiffness substrate. (F) Src inhibitor PP2 reduced the phosphorylation levels of Src, cortactin and the expression of Arg, cortactin and MMP14 in MHCC97H cells, but had little effect on the phosphorylation levels of EGFR and FAK. Data are representative images and expressed as mean \pm SD of each group from three separate experiments. *P < 0.05, **P < 0.01, ***P < 0.001, ****P < 0.0001.

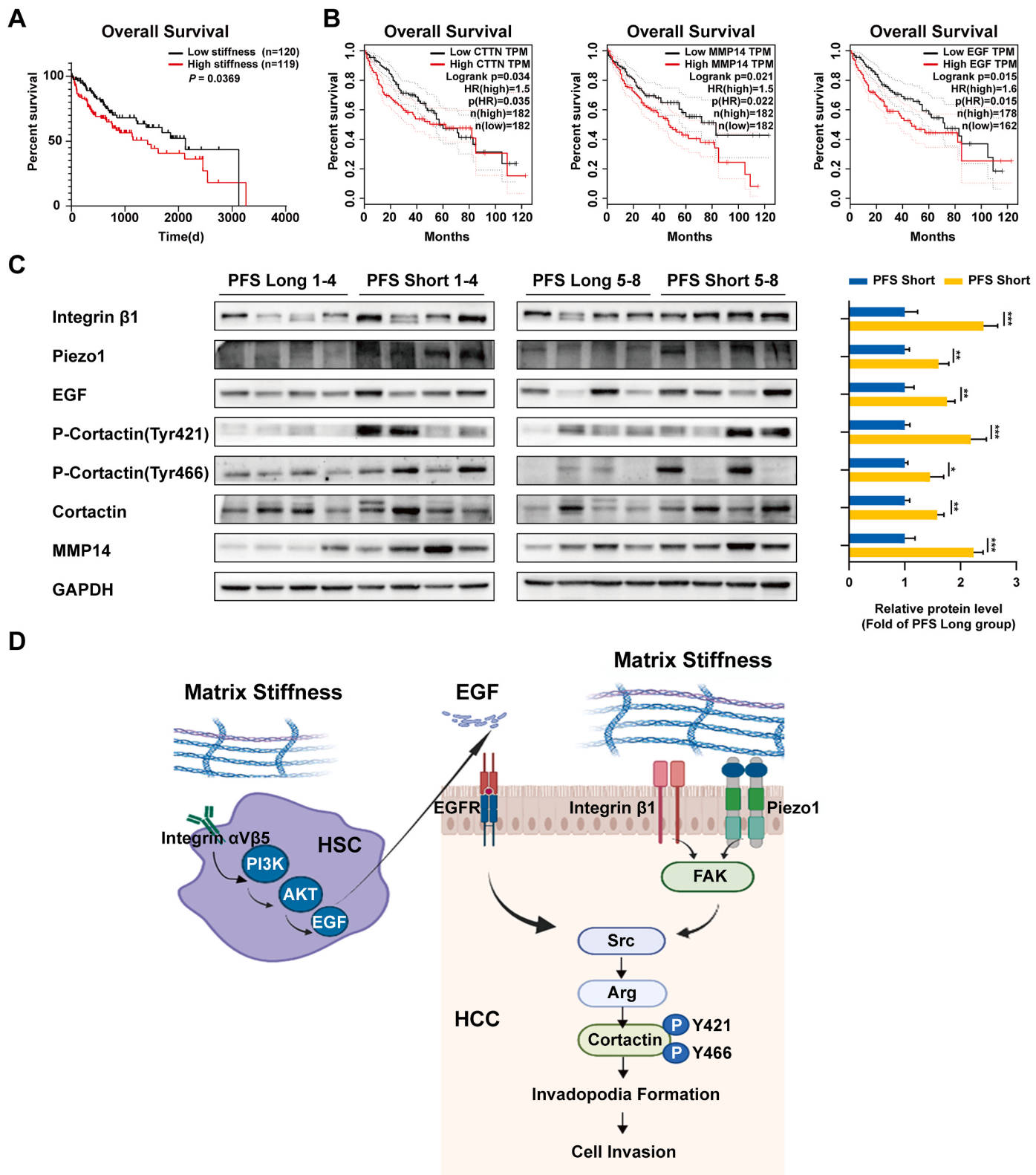


Fig. 7. Correlation between matrix stiffness and invadopodia-associated genes and its clinical significance. (A) TCGA-HCC analysis showed that the overall survival time of HCC patients in the high-stiffness group was significantly shorter than that in low-stiffness group. (B) TCGA-HCC analysis revealed that HCC patients in high cortactin, MMP14 and EGF expression group all had shorter overall survival than those in low cortactin, MMP14 and EGF expression group. (C) The expressions of integrin $\beta 1$, Piezo1, EGF, cortactin, MMP14 and the phosphorylation of cortactin (tyr421 and tyr466) in HCC tissue in short-PFS group were higher than those in HCC tissue in long-PFS group. Data are representative images and expressed as mean \pm SD of each group from three separate experiments. * $P < 0.05$, ** $P < 0.01$, *** $P < 0.001$. (D) The mechanism by which two pathways synergistically regulated matrix stiffness-driven invadopodia formation, including directly inducing invadopodia formation of HCC cells through activating integrin $\beta 1$ or Piezo1/FAK/Src/Arg/cortactin pathway, and indirectly stimulating invadopodia formation through improving hepatic stellate cells' EGF production to activate EGFR/Src/Arg/cortactin pathway.

Table 1

Associations of PFS with clinicopathologic characteristics in HCC patients.

Characteristics	Progression-free survival		P value
	Short (<24 months)	Long (> 24 months)	
No. of patients	42 (61.76 %)	26 (38.24 %)	
Gender			0.404
Male	32 (59.26 %)	22 (40.74 %)	
Female	10 (71.43 %)	4 (28.57 %)	
Age (years)	55.60 ± 10.58	52.96 ± 11.47	0.338
Liver stiffness (kPa)			0.007
≤8	7 (41.18 %)	10 (58.82 %)	
>8, <12	9 (47.37 %)	10 (52.63 %)	
≥12	26 (81.25 %)	6 (18.75 %)	
Tumor size (cm)	6.98 ± 4.79	6.50 ± 3.87	0.668
Tumor encapsulation			0.090
Yes	22 (53.66 %)	19 (46.34 %)	
No	20 (74.07 %)	7 (25.93 %)	
Microvascular invasion			0.048
Yes	28 (71.79 %)	11 (28.21 %)	
No	14 (48.28 %)	15 (51.72 %)	
Tumor differentiation			0.046
Edmondson I	0 (0.00 %)	3 (100.00 %)	
II-III	40 (63.49 %)	23 (36.51 %)	
IV	2 (100.00 %)	0 (0.00 %)	
Metavir's G grade			0.862
0	2 (50.00 %)	2 (50.00 %)	
1-2	36 (62.07)	22 (37.93)	
3	4 (66.67 %)	2 (33.33 %)	
Metavir's S grade			0.014
0-1	6 (40.00 %)	9 (60.00 %)	
2-3	8 (47.06 %)	9 (52.94 %)	
4	28 (77.78 %)	8 (22.22 %)	
AFP (ng/ml)	8282.62 ± 18409.37	2197.15 ± 4591.64	0.047
TB (μmol/l)	14.07 ± 7.84	12.80 ± 6.60	0.495
CB (μmol/l)	5.81 ± 5.63	4.92 ± 2.25	0.448
ALB (g/l)	42.81 ± 4.16	43.11 ± 3.92	0.770
ALP (U/l)	99.24 ± 70.83	85.19 ± 22.40	0.331
GGT (U/l)	115.93 ± 168.69	81.17 ± 60.60	0.317
ALT (U/l)	41.21 ± 46.97	35.33 ± 18.83	0.545
AST (U/l)	37.31 ± 33.66	31.02 ± 15.96	0.376
APTT (second)	25.310 ± 8.13	18.78 ± 10.92	0.012
PT (second)	19.31 ± 20.59	32.64 ± 39.88	0.074
GLU (mmol/l)	6.10 ± 2.68	5.47 ± 1.41	0.274

Abbreviations: AFP, alpha fetoprotein; TB, total bilirubin; CB, conjugated bilirubin; ALB, albumin; ALP, alkaline phosphatase; ALT, alanine aminotransferase; AST, aspartate aminotransferase; APTT, activated partial thromboplastin time; PT, prothrombin time; GLU, glucose.

integrin-FA-Lrp4/MuSK receptor pathway, thereby enhancing the malignant phenotype of HCC [38], implying that matrix stiffness may be an important reason for promoting the formation of invadopodia in HCC cells. Except for reinforcing the malignant characteristics of HCC cells, increased matrix stiffness also modulates the biological characteristics of other resident cells within tumor microenvironment [28,48]. HSCs activation is the most important contributor for liver fibrosis [44,49], and increasing matrix stiffness can continuously stimulate HSCs activation into tumor-promoting myofibroblasts [39,40]. Activated HSCs obviously facilitate tumor progression through secreting growth factors, ECM protein, cytokines [50,51]. More importantly, the released growth factors from activated HSCs such as EGF, TGF can exert strong inducing effect on the formation of invadopodia [41,52,53]. Thereby, there seems to be a linkage between matrix stiffness and invadopodia formation in HCC cells, and direct and indirect regulatory pathways may synergistically participate in matrix stiffness-driven invadopodia formation.

Given that high motility and invasion abilities of HCC cells can better represent invadopodia formation, we first evaluated the effects of matrix stiffness on cell motility/invasion ability and invadopodia-associated gene expression. Our results demonstrated that increased matrix stiffness significantly enhanced the motility and invasion abilities of HCC cells, and knockdown of mechanosensor partially weakened the motility and invasion phenotypes of HCC cells in high-stiffness environment. On

the other hand, increased matrix stiffness also evidently improved the number of invadopodia in HCC cells, and upregulated the expressions of invadopodia-associated genes (cortactin and MMP14), as well as the phosphorylation level of cortactin (Tyr421 and Tyr466). Analysis of TCGA-HCC tissues and buffalo rat HCC tissue microarray also confirmed an obviously high expressions in invadopodia-associated genes in high-stiffness group. Additionally, analysis of two types of HCC animal models also validated that downregulation of mechanosensor apparently suppressed the invasive ability of HCC cells and their invadopodia-associated genes expressions. These alterations in cell invasive phenotypes, the number of invadopodia and invadopodia-associated genes expression all support that a close linkage exists between matrix stiffness and invadopodia formation in HCC cells, and increased matrix stiffness promotes the formation of invadopodia. Interestingly, there was an obvious overexpression in EGF at the tissue level, but little change at the cell level, meaning that EGF overexpression at the tissue level may mainly come from the secretion of non-cancer cells within microenvironment. We speculated that biomechanical stimulation signal and paracrine-produced EGF might synergistically participate in matrix stiffness-driven invadopodia formation. EGF is a strong inducer for invadopodia formation of tumor cells [41,53]. EGF combined with EGFR can activate the non-receptor tyrosine kinase Arg to phosphorylate cortactin and trigger the polymerization and maturation of invasive pseudopodia actin [45], and EGFR-Src-Arg-cortactin pathway is involved in regulating the formation and activity of invasive pseudopodia in breast cancer cells [45]. In this study, exogenous stimulation of EGF distinctly increased the number of invadopodia formation in HCC cells grown on high-stiffness substrate, and increased matrix stiffness noticeably upregulated the expression of EGF in HSCs, confirming our speculation mentioned above. We further analyzed the synergistic mechanism of matrix stiffness and EGF in invadopodia formation of HCC cells, and discovered that direct and indirect regulatory pathways were involved in matrix stiffness-driven invadopodia formation together in HCC cells, including direct triggering invadopodia formation of HCC cells through activating integrin β1 or Piezo1/FAK/Src/Arg/cortactin pathway, and indirect stimulating invadopodia formation through improving EGF production of HSCs to activate EGFR/Src/Arg/cortactin pathway. Src was identified as the common hub molecule of two regulatory pathways (Fig. 7D).

Despite a synergistic regulation of matrix stiffness and paracrine-released EGF in invadopodia formation is clearly clarified in the study, we are still unable to exclude the contribution of matrix stiffness combining with other paracrine cytokines to invadopodia formation. Additionally, the detailed interplay between integrin β1-based and Piezo1-based mechanosensory in invadopodia formation also merits to be further investigated in the following study.

This study disclosed a new mechanism by which mechanosensory pathway and biochemical signal pathway synergistically promoted the formation of invadopodia in HCC cells. Our findings undoubtedly enrich the regulatory theory of increased matrix stiffness-strengthened invasion and metastasis, and offer a new intervention perspective targeting on matrix stiffness in HCC.

Funding

The present study was supported by a grant from the National Natural Science Foundation of China (Grant No. 81972910).

Data availability

All the research material and data reported in the article are available upon request to the authors.

Ethics approval and consent to participate

The study was approved by the Zhongshan Hospital Research Ethics

Committee (Approval No. B2020-018R). Written informed consent was obtained from all patients. All animal care and experiments used in this study were in accordance with the guideline for the Care and Use of Laboratory Animals published by the US National Academy of Science (Washington, WA, USA), and the related experiment design met with approval from the Animal Care Ethical Committee of Zhongshan Hospital, Fudan University (Shanghai, China) (Approval No. 2020-116).

CRediT authorship contribution statement

Xi Zhang: Writing – original draft, Visualization, Validation, Software, Project administration, Methodology, Investigation, Formal analysis, Data curation. **Yingying Zhao:** Writing – original draft, Visualization, Validation, Software, Project administration, Methodology, Investigation, Formal analysis, Data curation. **Miao Li:** Writing – original draft, Visualization, Validation, Software, Project administration, Methodology, Investigation, Formal analysis, Data curation. **Mimi Wang:** Software, Project administration, Data curation. **Jiali Qian:** Software, Project administration, Investigation. **Zhiming Wang:** Project administration, Methodology. **Yaohui Wang:** Validation, Project administration, Formal analysis, Data curation. **Fan Wang:** Supervision. **Kun Guo:** Supervision. **Dongmei Gao:** Supervision, Resources, Methodology. **Yan Zhao:** Supervision, Resources. **Rongxin Chen:** Supervision, Resources, Methodology. **Zhenggang Ren:** Supervision, Resources, Methodology. **Haiyan Song:** Writing – review & editing, Supervision, Resources, Methodology, Conceptualization. **Jiefeng Cui:** Writing – review & editing, Supervision, Resources, Methodology, Funding acquisition, Conceptualization.

Declaration of competing interest

The authors declare that they have no known competing financial interests or personal relationships that could have appeared to influence the work reported in this paper.

Acknowledgements

We are grateful to Dr. Yanyu Jiang (Longhua Hospital, Shanghai University of Traditional Chinese Medicine) for kindly guiding the use of laser confocal microscope.

Appendix A. Supplementary data

Supplementary data to this article can be found online at <https://doi.org/10.1016/j.canlet.2023.216597>.

References

- [1] S. Linder, P. Cervero, R. Eddy, J. Condeelis, Mechanisms and roles of podosomes and invadopodia, *Nat. Rev. Mol. Cell Biol.* 24 (2023) 86–106.
- [2] R.J. Eddy, M.D. Weidmann, V.P. Sharma, J.S. Condeelis, Tumor cell invadopodia: invasive protrusions that orchestrate metastasis, *Trends Cell Biol.* 27 (2017) 595–607.
- [3] T. Mgirditchian, G. Sakalauskaite, T. Müller, C. Hoffmann, C. Thomas, The multiple roles of actin-binding proteins at invadopodia, *Int. Rev. Cell Mol. Biol.* 360 (2021) 99–132.
- [4] Y. Moshfegh, J.J. Bravo-Cordero, V. Miskolci, J. Condeelis, L. Hodgson, A Trio-Rac1-Pak1 signalling axis drives invadopodia disassembly, *Nat. Cell Biol.* 17 (2015) 350.
- [5] H. Yamaguchi, Pathological roles of invadopodia in cancer invasion and metastasis, *Eur. J. Cell Biol.* 91 (2012) 902–907.
- [6] H. Yamaguchi, M. Lorenz, S. Kempfak, C. Sarmiento, S. Coniglio, M. Symons, J. Segall, R. Eddy, H. Miiki, T. Takenawa, J. Condeelis, Molecular mechanisms of invadopodium formation: the role of the N-WASP-Arp2/3 complex pathway and cofilin, *J. Cell Biol.* 168 (2005) 441–452.
- [7] V.P. Sharma, R. Eddy, D. Entenberg, M. Kai, F.B. Gertler, J. Condeelis, Tks5 and SHIP2 regulate invadopodium maturation, but not initiation, in breast carcinoma cells, *Curr. Biol.* 23 (2013) 2079–2089.
- [8] C.L. Cortesio, K.T. Chan, B.J. Perrin, N.O. Burton, S. Zhang, Z.Y. Zhang, A. Huttenlocher, Calpain 2 and PTP1B function in a novel pathway with Src to regulate invadopodia dynamics and breast cancer cell invasion, *J. Cell Biol.* 180 (2008) 957–971.
- [9] P.J. van Haastert, I. Keizer-Gunnink, A. Kortholt, Coupled excitable Ras and F-actin activation mediates spontaneous pseudopod formation and directed cell movement, *Mol. Biol. Cell* 28 (2017) 922–934.
- [10] H. Nakahara, T. Otani, T. Sasaki, Y. Miura, Y. Takai, M. Kogo, Involvement of Cdc42 and Rac small G proteins in invadopodia formation of RPMI7951 cells, *Gene Cell.* 8 (2003) 1019–1027.
- [11] K.E. Pourfarhangi, A. Bergman, B. Gligorijevic, ECM cross-linking regulates invadopodia dynamics, *Biophys. J.* 114 (2018) 1455–1466.
- [12] B. Diaz, A. Yuen, S. Iizuka, S. Higashiyama, S.A. Courtneidge, Notch increases the shedding of HB-EGF by ADAM12 to potentiate invadopodia formation in hypoxia, *J. Cell Biol.* 201 (2013) 279–292.
- [13] X. Peng, X. Li, S. Yang, M. Huang, S. Wei, Y. Ma, Y. Li, B. Wu, H. Jin, B. Li, S. Tang, Q. Fan, J. Liu, L. Yang, H. Li, LINC00511 drives invasive behavior in hepatocellular carcinoma by regulating exosome secretion and invadopodia formation, *J. Exp. Clin. Cancer Res.* 40 (2021) 183.
- [14] O.Y. Revach, I. Grosheva, B. Geiger, Biomechanical regulation of focal adhesion and invadopodia formation, *J. Cell Sci.* 133 (2020).
- [15] N.R. Alexander, K.M. Branch, A. Parekh, E.S. Clark, I.C. Iwueke, S.A. Guelcher, A. M. Weaver, Extracellular matrix rigidity promotes invadopodia activity, *Curr. Biol.* 18 (2008) 1295–1299.
- [16] R.J. Jerrell, A. Parekh, Matrix rigidity differentially regulates invadopodia activity through ROCK1 and ROCK2, *Biomaterials* 84 (2016) 119–129.
- [17] H. Mohammadi, E. Sahai, Mechanisms and impact of altered tumour mechanics, *Nat. Cell Biol.* 20 (2018) 766–774.
- [18] J. Schrader, T.T. Gordon-Walker, R.L. Aucott, M. van Deemter, A. Quaas, S. Walsh, D. Benten, S.J. Forbes, R.G. Wells, J.P. Iredale, Matrix stiffness modulates proliferation, chemotherapeutic response, and dormancy in hepatocellular carcinoma cells, *Hepatology* 53 (2011) 1192–1205.
- [19] G. Zhao, J. Cui, Q. Qin, J. Zhang, L. Liu, S. Deng, C. Wu, M. Yang, S. Li, C. Wang, Mechanical stiffness of liver tissues in relation to integrin $\beta 1$ expression may influence the development of hepatic cirrhosis and hepatocellular carcinoma, *J. Surg. Oncol.* 102 (2010) 482–489.
- [20] N. Li, X. Zhang, J. Zhou, W. Li, X. Shu, Y. Wu, M. Long, Multiscale biomechanics and mechanotransduction from liver fibrosis to cancer, *Adv. Drug Deliv. Rev.* 188 (2022), 114448.
- [21] Y. Dong, Q. Zheng, Z. Wang, X. Lin, Y. You, S. Wu, Y. Wang, C. Hu, X. Xie, J. Chen, D. Gao, Y. Zhao, W. Wu, Y. Liu, Z. Ren, R. Chen, J. Cui, Higher matrix stiffness as an independent initiator triggers epithelial-mesenchymal transition and facilitates HCC metastasis, *J. Hematol. Oncol.* 12 (2019) 112.
- [22] N. Yang, T. Chen, L. Wang, R. Liu, Y. Niu, L. Sun, B. Yao, Y. Wang, W. Yang, Q. Liu, K. Tu, Z. Liu, CXCR4 mediates matrix stiffness-induced downregulation of UBDT1 driving hepatocellular carcinoma progression via YAP signaling pathway, *Theranostics* 10 (2020) 5790–5801.
- [23] M. Li, X. Zhang, M. Wang, Y. Wang, J. Qian, X. Xing, Z. Wang, Y. You, K. Guo, J. Chen, D. Gao, Y. Zhao, L. Zhang, R. Chen, J. Cui, Z. Ren, Activation of Piez1 contributes to matrix stiffness-induced angiogenesis in hepatocellular carcinoma, *Cancer Commun.* 42 (2022) 1162–1184.
- [24] Y. Dong, X. Xie, Z. Wang, C. Hu, Q. Zheng, Y. Wang, R. Chen, T. Xue, J. Chen, D. Gao, W. Wu, Z. Ren, J. Cui, Increasing matrix stiffness upregulates vascular endothelial growth factor expression in hepatocellular carcinoma cells mediated by integrin beta1, *Biochem. Biophys. Res. Commun.* 444 (2014) 427–432.
- [25] Y. Wang, X. Zhang, W. Wang, X. Xing, S. Wu, Y. Dong, Y. You, R. Chen, Z. Ren, W. Guo, J. Cui, W. Li, Integrin alphaVbeta5/Akt/Spl pathway participates in matrix stiffness-mediated effects on VEGFR2 upregulation in vascular endothelial cells, *Am. J. Cancer Res.* 10 (2020) 2635–2648.
- [26] S. Wu, X. Xing, Y. Wang, X. Zhang, M. Li, M. Wang, Z. Wang, J. Chen, D. Gao, Y. Zhao, R. Chen, Z. Ren, K. Zhang, J. Cui, The pathological significance of LOXL2 in pre-metastatic niche formation of HCC and its related molecular mechanism, *Eur. J. Cancer* 147 (2021) 63–73.
- [27] S. Wu, Q. Zheng, X. Xing, Y. Dong, Y. Wang, Y. You, R. Chen, C. Hu, J. Chen, D. Gao, Y. Zhao, Z. Wang, T. Xue, Z. Ren, J. Cui, Matrix stiffness-upregulated LOXL2 promotes fibronectin production, MMP9 and CXCL12 expression and BMDCs recruitment to assist pre-metastatic niche formation, *J. Exp. Clin. Cancer Res.* 37 (2018) 99.
- [28] X. Xing, Y. Wang, X. Zhang, X. Gao, M. Li, S. Wu, Y. Zhao, J. Chen, D. Gao, R. Chen, Z. Ren, K. Zhang, J. Cui, Matrix stiffness-mediated effects on macrophages polarization and their LOXL2 expression, *FEBS J.* 288 (2021) 3465–3477.
- [29] Y. You, Q. Zheng, Y. Dong, X. Xie, Y. Wang, S. Wu, L. Zhang, Y. Wang, T. Xue, Z. Wang, R. Chen, Y. Wang, J. Cui, Z. Ren, Matrix stiffness-mediated effects on stemness characteristics occurring in HCC cells, *Oncotarget* 7 (2016) 32221–32231.
- [30] W. Zhao, H. Mo, R. Liu, T. Chen, N. Yang, Z. Liu, Matrix stiffness-induced upregulation of histone acetyltransferase KAT6A promotes hepatocellular carcinoma progression through regulating SOX2 expression, *Br. J. Cancer* 127 (2022) 202–210.
- [31] D. Lachowski, C. Matellan, S. Gopal, E. Cortes, B.K. Robinson, A. Saiani, A. F. Miller, M.M. Stevens, A.E. Del Río Hernández, Substrate stiffness-driven membrane tension modulates vesicular trafficking via caveolin-1, *ACS Nano* 16 (2022) 4322–4337.
- [32] B. Wu, D.A. Liu, L. Guan, P.K. Myint, L. Chin, H. Dang, Y. Xu, J. Ren, T. Li, Z. Yu, S. Jabban, G.B. Mills, J. Nukpezah, Y.H. Chen, E.E. Furth, P.A. Gimotty, R.G. Wells, V.M. Weaver, R. Radhakrishnan, X.W. Wang, W. Guo, Stiff matrix induces exosome secretion to promote tumour growth, *Nat. Cell Biol.* 25 (2023) 415–424.

- [33] S. Wang, L. Chen, W. Liu, Matrix stiffness-dependent STEAP3 coordinated with PD-L2 identify tumor responding to sorafenib treatment in hepatocellular carcinoma, *Cancer Cell Int.* 22 (2022) 318.
- [34] H.H. Liu, Y. Xu, C.J. Li, S.J. Hsu, X.H. Lin, R. Zhang, J. Chen, J. Chen, D.M. Gao, J. F. Cui, X.R. Yang, Z.G. Ren, R.X. Chen, An SCD1-dependent mechanoresponsive pathway promotes HCC invasion and metastasis through lipid metabolic reprogramming, *Mol. Ther.* 30 (2022) 2554–2567.
- [35] C. Liu, Y. Liu, H.G. Xie, S. Zhao, X.X. Xu, L.X. Fan, X. Guo, T. Lu, G.W. Sun, X.J. Ma, Role of three-dimensional matrix stiffness in regulating the chemoresistance of hepatocellular carcinoma cells, *Biotechnol. Appl. Biochem.* 62 (2015) 556–562.
- [36] X. Gao, X. Qiao, X. Xing, J. Huang, J. Qian, Y. Wang, Y. Zhang, X. Zhang, M. Li, J. Cui, Y. Yang, Matrix stiffness-upregulated MicroRNA-17-5p attenuates the intervention effects of metformin on HCC invasion and metastasis by targeting the PTEN/PI3K/Akt pathway, *Front. Oncol.* 10 (2020) 1563.
- [37] S. Chakraborty, M. Lakshmanan, H.L. Swa, J. Chen, X. Zhang, Y.S. Ong, L.S. Loo, S. C. Akincilar, J. Gunaratne, V. Tergaonkar, K.M. Hui, W. Hong, An oncogenic role of Agrin in regulating focal adhesion integrity in hepatocellular carcinoma, *Nat. Commun.* 6 (2015) 6184.
- [38] S. Chakraborty, K. Njah, A.V. Pobbat, Y.B. Lim, A. Raju, M. Lakshmanan, V. Tergaonkar, C.T. Lim, W. Hong, Agrin as a mechanotransduction signal regulating YAP through the hippo pathway, *Cell Rep.* 18 (2017) 2464–2479.
- [39] Z. Liu, H. Mo, R. Liu, Y. Niu, T. Chen, Q. Xu, K. Tu, N. Yang, Matrix stiffness modulates hepatic stellate cell activation into tumor-promoting myofibroblasts via E2F3-dependent signaling and regulates malignant progression, *Cell Death Dis.* 12 (2021) 1134.
- [40] C. Dou, Z. Liu, K. Tu, H. Zhang, C. Chen, U. Yaqoob, Y. Wang, J. Wen, J. van Deursen, D. Sicard, D. Tschumperlin, H. Zou, W.C. Huang, R. Urrutia, V.H. Shah, N. Kang, P300 acetyltransferase mediates stiffness-induced activation of hepatic stellate cells into tumor-promoting myofibroblasts, *Gastroenterology* 154 (2018) 2209–2221, e2214.
- [41] V. Desmarais, H. Yamaguchi, M. Oser, L. Soon, G. Mouneimne, C. Sarmiento, R. Eddy, J. Condeelis, N-WASP and cortactin are involved in invadopodium-dependent chemotaxis to EGF in breast tumor cells, *Cell Motil Cytoskeleton* 66 (2009) 303–316.
- [42] P. Jeannot, A. Nowosad, R.T. Perchey, C. Callot, E. Bennana, T. Katsume, P. Mayeux, F. Guillonneau, S. Manenti, A. Besson, p27(Kip1) promotes invadopodia turnover and invasion through the regulation of the PAK1/Cortactin pathway, *Elife* 6 (2017).
- [43] C. Cui, R. Merritt, L. Fu, Z. Pan, Targeting calcium signaling in cancer therapy, *Acta Pharm. Sin. B* 7 (2017) 3–17.
- [44] C. Yang, M. Zeisberg, B. Mosterman, A. Sudhakar, U. Yerramalla, K. Holthaus, L. Xu, F. Eng, N. Afshar, R. Kalluri, Liver fibrosis: insights into migration of hepatic stellate cells in response to extracellular matrix and growth factors, *Gastroenterology* 124 (2003) 147–159.
- [45] C.C. Mader, M. Oser, M.A. Magalhaes, J.J. Bravo-Cordero, J. Condeelis, A. J. Koleske, H. Gil-Henn, An EGFR-Src-Arg-cortactin pathway mediates functional maturation of invadopodia and breast cancer cell invasion, *Cancer Res.* 71 (2011) 1730–1741.
- [46] D. Gianni, N. Taulet, C. DerMardirossian, G.M. Bokoch, c-Src-mediated phosphorylation of Nox1 and Tks4 induces the reactive oxygen species (ROS)-dependent formation of functional invadopodia in human colon cancer cells, *Mol. Biol. Cell* 21 (2010) 4287–4298.
- [47] B.T. Beaty, V.P. Sharma, J.J. Bravo-Cordero, M.A. Simpson, R.J. Eddy, A. J. Koleske, J. Condeelis, beta1 integrin regulates Arg to promote invadopodial maturation and matrix degradation, *Mol. Biol. Cell* 24 (2013) 1661–1675, S1661–1611.
- [48] D. Lachowski, E. Cortes, A. Rice, D. Pinato, K. Rombouts, A. Del Rio Hernandez, Matrix stiffness modulates the activity of MMP-9 and TIMP-1 in hepatic stellate cells to perpetuate fibrosis, *Sci. Rep.* 9 (2019) 7299.
- [49] T. Tsuchida, S.L. Friedman, Mechanisms of hepatic stellate cell activation, *Nat. Rev. Gastroenterol. Hepatol.* 14 (2017) 397–411.
- [50] J.J. Loh, T.W. Li, L. Zhou, T.L. Wong, X. Liu, V.W.S. Ma, C.M. Lo, K. Man, T.K. Lee, W. Ning, M. Tong, S. Ma, FSTL1 secreted by activated fibroblasts promotes hepatocellular carcinoma metastasis and stemness, *Cancer Res.* 81 (2021) 5692–5705.
- [51] Y. Myojin, H. Hikita, M. Sugiyama, Y. Sasaki, K. Fukumoto, S. Sakane, Y. Makino, N. Takemura, R. Yamada, M. Shigekawa, T. Kodama, R. Sakamori, S. Kobayashi, T. Tatsumi, H. Suemizu, H. Eguchi, N. Kokudo, M. Mizokami, T. Takehara, Hepatic stellate cells in hepatocellular carcinoma promote tumor growth via growth differentiation factor 15 production, *Gastroenterology* 160 (2021) 1741–1754, e1716.
- [52] Z. Chen, S. He, Y. Zhan, A. He, D. Fang, Y. Gong, X. Li, L. Zhou, TGF-beta-induced transgelin promotes bladder cancer metastasis by regulating epithelial-mesenchymal transition and invadopodia formation, *EBioMedicine* 47 (2019) 208–220.
- [53] A. Makowiecka, A. Simiczyjew, D. Nowak, A.J. Mazur, Varying effects of EGF, HGF and TGFbeta on formation of invadopodia and invasiveness of melanoma cell lines of different origin, *Eur. J. Histochem.* 60 (2016) 2728.